

ZİRVE UNIVERSITY

REAL-TIME MONITORING OF A STEEL BUILDING AND ITS
PERFORMANCE ANALYSIS

by

Abdullahi SAGIR

Submitted to the Institute for Graduate Studies in
Natural and Applied Sciences in partial fulfillment of
the requirements for the degree of
Master of Science

Graduate Program in Civil Engineering
Thesis Supervisor: Assoc. Prof. Dr. M. Cemal GENES

June, 2014

REAL-TIME MONITORING OF A STEEL BUILDING AND ITS
PERFORMANCE ANALYSIS

APPROVED BY:

Assoc. Prof. Dr. M. Cemal GENES
(Thesis Supervisor)

Assoc. Prof. Dr. Abdulkadir CEVIK

Assoc. Prof. Dr. Mahmut BILGEHAN

Prof. Dr. Sinan HINISLIOĞLU
Director of Graduate School of Natural and Applied Sciences

Abdullahi SAGIR June, 2014

All Rights Reserved

ACKNOWLEDGEMENTS

This study was conducted under the supervision of Assoc. Prof. Dr. M. Cemal GENES. I would like to express my sincere appreciation for the support, guidance and insights that he has provided me throughout the study. In the course of preparing this study and indeed all the way before now, a great number of people have helped me along the way, in forms of materials, ideas, and support despite their busy and tight schedule, it's really appreciated.

I must not forget Assoc. Prof. Dr. Mahmut BILGEHAN, Head of Civil Engineering Department Zirve University, Assoc. Prof. Dr. Ismail HALTAS Civil Engineering Department Zirve University and PhD. Student Ismail Ozan Demirel at Middle East Technical University for their generous assistance. Finally. I would like to thanks my friends both at school and home, who have kept my spirit up and assisted me for their diligence and efficiency, and I close by giving yet more thanks, quite appropriately to Allah (S.W.T).

ABSTRACT

REAL-TIME MONITORING OF A STEEL BUILDING AND ITS PERFORMANCE ANALYSIS

Abdullahi SAGIR

ZİRVE UNIVERSITY

GRADUATE SCHOOL OF NATURAL AND APPLIED SCIENCES

Thesis Supervisor: Assoc. Prof. Dr. M. Cemal GENES

In this thesis, a 6-story, steel building with reinforced concrete (R/C) core shear walls, were instrumented with 12 uni-axial accelerometers, which is intended for Structural Health Monitoring (SHM) with aims of providing in real-time informations regarding to the health of the building. The response of the building to ambient vibration from ground and wind were recorded by the sensitive accelerometers continuously. Three different readings were selected from the continuous readings and analyzed, the dynamic properties obtained from the readings were compared with each other. A 3D-Finite Element Model (FEM) of the instrumented building was prepared and the analytical results obtained from modal analysis were compared with the experimental results and the formula given in the code. Nonlinear pushover analysis was performed on the analytical model to obtained the pushover curve and the performance point. The performance point showed that the structure is expected to show a good performance under severe earthquakes.

Keywords: Structural Health Monitoring, Seismic Instrumentation, Pushover Analysis, Performance Analysis.

ÖZET

ÇELİK BİR BİNANIN GERÇEK-ZAMANLI OLARAK İZLENMESİ VE PERFORMANS ANALİZİ

Abdullahi SAGIR

ZİRVE ÜNİVERSİTESİ

FEN BİLİMLERİ ENSTİTÜSÜ

Tez Danışmanı: Assoc. Prof. Dr. M. Cemal GENES

Bu tezde, betonarme çekirdeği bulunan 6 katlı çelik bir binanın yapı sağlığının gerçek-zamanlı olarak takibi amacıyla 12 adet tek-eksenli ivmeölçer ile donatılmıştır. Binada zeminden gelen ve rüzgardan dolayı oluşan titreşimler, hassas ivmeölçerler ile sürekli olarak ölçülmüştür. Kayıt edilen titreşimlerden, üç titreşim kaydı seçilmiş ve analiz edilmiş, binanın takibi amacıyla elde edilen dinamik davranış özellikleri birbiri ile karşılaştırılmıştır. Deprem cihazları ile donatılmış binanın 3-Botutlu Sonlu Elemanlar Modeli hazırlanmış ve modal analizden elde edilen analitik sonuçlar deneysel sonuçlar ile ve deprem yönetmeliğindeki formül ile karşılaştırılmıştır. Binanın statik itme eğrisinin ve performans noktasının belirlenmesi amacıyla, analitik model üzerinde doğrusal olmayan statik-itme analizi gerçekleştirilmiştir. Performans noktasına göre yapının siddetli deprem etkisi altında iyi performans göstereceği görülmüştür.

Anahtar Kelimeler: Yapı Sağlığı Takibi, Sismik instrumentasyon, Statik itme analizi, Performans analizi.

TABLE OF CONTENTS

ACKNOWLEDGEMENTS	iv
ABSTRACT	v
ÖZET	vi
LIST OF FIGURES	ix
LIST OF TABLES	xiv
1. INTRODUCTION	1
1.1. Introduction	1
1.2. Aim of the Study	2
1.3. Objectives of the Study	2
1.4. Scope of the Study	3
2. LITERATURE REVIEW	4
2.1. Seismic Instrumentation of Buildings	4
2.2. Steps in Instrumenting a Structure	5
2.2.1. Selection of Structure to be Instrumented	5
2.2.2. Selection and Installation of Instruments	8
2.2.3. Maintenance	13
2.2.4. Testing, Measurement, and Post Processing of Recorded Data	13
2.2.5. Comparison Against FEM and Evaluation	14
2.3. Previous Studies on Structural Health Monitoring and Performance Analysis	15
3. EXPERIMENTAL STUDY AND DATA ANALYSIS	19
3.1. Introduction	19
3.2. Selection of Structure to be Instrumented	19
3.3. Selection and Installation of Instruments	25
3.3.1. Strong Motion Accelerometer	26
3.3.2. Data Acquisition System	27
3.3.3. Scream Software	29
3.3.4. Installation Process	32
3.4. Post Processing of the Recorded Data	33

3.4.1. Fourier Analysis	35
3.4.2. Fast Fourier Transform	35
3.4.3. FFT Application on the Recorded Data	38
3.4.4. Analysis of Ambient Data Recorded on (Nov. 11, 2013)	38
3.4.5. Analysis of an Earthquake Data Recorded on (Feb. 14, 2014)	42
3.4.6. Analysis of Ambient Data Recorded on (March 1, 2014)	46
3.5. Discussion of Experimental Results	50
4. ANALYTICAL STUDY	52
4.1. Introduction	52
4.2. Finite Element Model (FEM)	52
4.3. Comparison Between Experimental Results, Analytical Finite Element Model (FEM) and Code Formula	55
4.4. Pushover Analysis	57
4.5. Performance Levels of Structures and Elements	59
4.5.1. Immediate Occupancy (IO)	59
4.5.2. Life Safety (LS)	60
4.5.3. Collapse Prevention (CP)	60
4.6. Pushover Analysis of the Instrumented Building	60
5. CONCLUSIONS AND RECOMMENDATIONS	65
5.1. Summary	65
5.2. Conclusions	66
5.3. Recommendations	66
REFERENCES	67
APPENDIX A:	70

LIST OF FIGURES

Figure 2.1.	(From left to the right) Uni-axial, Tri-axial and Down-hole Forced-Balanced Accelerometers [3]	8
Figure 2.2.	View of the force balance accelerometer (Episensor) [4]	9
Figure 2.3.	View of the 24-bit strong motion accelerograph [5]	9
Figure 2.4.	View of the geometrics 24 channel geode seismograph [6]	10
Figure 2.5.	Schematic diagram showing typical deployment of sensors and routing of cables to the recorder [3]	12
Figure 3.1.	Six-story steel hinged-framed building	20
Figure 3.2.	Foundation connection (Rigid connection)	21
Figure 3.3.	Beam to beam hinge connection [12]	21
Figure 3.4.	Ground floor plan view showing the distribution of steel columns and central shear walls	22
Figure 3.5.	Typical (1st to 5th) floors of the building, showing the distribution of steel columns and central shear walls	22
Figure 3.6.	Section cutting through the building, showing the distribution of steel columns, beams as well as the central core shear wall	23
Figure 3.7.	Earthquake faults region [13]	24

Figure 3.8.	Showing the building-free located away from the main building . . .	25
Figure 3.9.	CMG-5U Strong motion accelerometer	26
Figure 3.10.	Data acquisition system, located in the cabinet for safety	27
Figure 3.11.	Graphical view of 12 recording channels data, using Scream Software	31
Figure 3.12.	View of the (12 recording channels) in Scream Software	31
Figure 3.13.	Schematic view of the building depicting location as well as the orientation of the 12 accelerometers in the building and free-field (The arrows indicating the orientation of positive acceleration for each sensors)	32
Figure 3.14.	Location of the recorded earthquake, Feb 14, 2014 at 02:33am [15]	34
Figure 3.15.	Graphical User Interface (GUI) of the program writing in MAT- LAB, for Data Processing in Real-Time	35
Figure 3.16.	Displacement plot of the top three sensors (Top Layer) in meters .	38
Figure 3.17.	Displacement plot of the three sensors in the fourth floor, in meters	39
Figure 3.18.	Displacement plot of the three sensors in second the second floor, in meters	39
Figure 3.19.	Fourier Amplitude plot of the top sensors, sixth floor (x-direction). The first plot is CH10 and CH11, the second plot is CH12. The third plot is (CH10+CH11) and (CH10-CH11) for torsion detec- tion in the building	40

Figure 3.20. Fourier Amplitude plot of the sensors in fourth floor (y-direction). The first plot is CH7 and CH9, the second plot is CH8. The third plot is (CH7+CH9) and (CH7-CH9) for torsion detection in the building	40
Figure 3.21. Fourier Amplitude plot of the sensors in second floor (x-direction). The first plot is CH4 and CH5, the second plot is CH6. The third plot is (CH4+CH5) and (CH4-CH5) for torsion detection in the building	41
Figure 3.22. Displacement plot of the top three sensors (top layer) in meters . .	42
Figure 3.23. Displacement plot of the three sensors in the fourth floor, in meters	42
Figure 3.24. Displacement plot of the three sensors in the second floor, in meters	43
Figure 3.25. Displacement of the three sensors in the free-field station, in meters	43
Figure 3.26. Fourier Amplitude plot of the top sensors, six floor (x-direction). The first plot is CH10 and CH11, the second plot is CH12. The third plot is (CH10+CH11) and (CH10-CH11) for torsion detec- tion in the building	44
Figure 3.27. Fourier Amplitude plot of the sensors in fourth floor (y-direction). The first plot is CH7 and CH9, the second plot is CH8. The third plot is (CH7+CH9) and (CH7-CH9) for torsion detection in the building	44
Figure 3.28. Fourier Amplitude plot of the sensors in second floor (x-direction). The first plot is CH4 and CH5, the second plot is CH6. The third plot is (CH4+CH5) and (CH4-CH5) for torsion detection in the building	45

Figure 3.29.	Displacement plot of the top three sensors (top layer) in meters . . .	46
Figure 3.30.	Displacement plot of the three sensors in fourth floor, in meters . . .	46
Figure 3.31.	Displacement plot of the three sensors in second floor, in meters . . .	47
Figure 3.32.	Displacement plot of the three sensors in free-field station, in meters . . .	47
Figure 3.33.	Fourier Amplitude plot of the top three sensors, sixth floor (x-direction). The first plot is CH10 and CH11, the second plot is CH12. The third plot is (CH10+CH11) and (CH10-CH11) for torsion detection in the building	48
Figure 3.34.	Fourier Amplitude plot of the sensors in fourth floor (y-direction). The first plot is CH7 and CH9, the second plot is CH8. The third plot is (CH7+CH9) and (CH7-CH9) for torsion detection in the building	48
Figure 3.35.	Fourier Amplitude plot of the sensors in second floor (x-direction). The first plot is CH4 and CH5, the second plot is CH6. The third plot is (CH4+CH5) and (CH4-CH5) for torsion detection in the building	49
Figure 4.1.	Three dimensional physical model of the instrumented building . . .	53
Figure 4.2.	Fundamental mode shape of the instrumented building in y-direction . . .	54
Figure 4.3.	Fundamental mode shape of the instrumented building in x-direction . . .	54
Figure 4.4.	Performance point of a structure	58
Figure 4.5.	Performance levels as per FEMA 356	59

Figure 4.6.	Three dimensional analytical model of the instrumented building .	61
Figure 4.7.	Mid-Pier model for shear wall	61
Figure 4.8.	Pushover curve of the instrumented building	62
Figure 4.9.	Story drift ratio of the instrumented building	63
Figure 4.10.	Performance point of the instrumented steel building	63
Figure 4.11.	Plastic hinges of the instrumented building in x-direction	64

LIST OF TABLES

Table 3.1.	Summary of the ambient/earthquake data recorded from the building	33
Table 3.2.	Summary of the experimental results obtained from the building, using ambient data	41
Table 3.3.	Summary of the experimental results obtained from the building, using earthquake data	45
Table 3.4.	Summary of the experimental results obtained from the building, using ambient data	49
Table 3.5.	Summary of the experimental results obtained from the three sets of data	50
Table 4.1.	Summary of the modal analysis result obtained from the analysis model	53
Table 4.2.	Comparison of frequencies (Periods) from Fourier analyses, Finite Element Model and Code Formula	57

1. INTRODUCTION

1.1. Introduction

Building as a structural system is one of the complex engineered system that ensure society's economic and industrial prosperity. To design buildings that are safe for public use, standardized building codes and design methodologies have been created [1]. Unfortunately buildings are often subjected to harsh loadings scenarios and severe environmental conditions which are not well anticipated during design process that will result in long-term structural deterioration. Recent seismic events in Turkey (Marmara, Duzce, Bingol and Van), reveals buildings vulnerability to damage and failure during natural catastrophes. To design safer and more durable structures, the engineering community is aggressively pursuing novel sensing technologies and analytical methods that can be used to rapidly identify the onsets of structural damages in an instrumented structural system [1], called Structural Health Monitoring (SHM). This paradigm offers an automated method for tracking the health of structures by combining damage detection algorithms with structural monitoring systems.

Structural Health Monitoring is used for rapid condition screening and aims to provide, in near real-time reliable information regarding the integrity of the structure. Structural monitoring systems are widely adopted to monitor the behavior of structures during forced vibration testing or natural excitations (e.g., earthquake, wind, and live loading etc.). Structural monitoring systems can be found in a numbers of common structures including civil structures, air craft's, and ships. For example, some building design codes mandate that for structures located in regions of high seismic activity have structural monitoring systems installed [2]. The monitoring system is primarily responsible for collecting the measurement output from sensors installed in the structure and storing the measured data within a central data repository before the processing take place.

The purpose of this thesis is to monitor a six-story steel building located in Antakya (Turkey), which is instrumented with 12-channels Health Monitoring System that streams real-time acceleration data from different floors in order to find its dy-

dynamic properties. The dynamic properties of the building obtained from the recorded data are found to compare well with each other, so that to investigate the differences between them. Also Finite Element Model (FEM) of the building were constructed, the dynamic properties determined from model analyses using a Finite Element Model were compared with the result obtained from the experimented data and the formula given in the Turkish earthquake code. Nonlinear pushover analysis was performed on the analytical model and the pushover curves and the performance point were obtained, the performance point showed that the structure will perform well under earthquake.

The result of such comparisons helps to better understand the performance level of a steel building. The obtained result will help to improve the design and construction technology of steel buildings, in order to reduce the loss of lives and properties during strong earthquakes, also the obtained results will be a contribution to the ongoing researches in this area.

1.2. Aim of the Study

This thesis is essentially a study of performances analysis of buildings, more particularly steel building located in a seismic zone. It is an attempt of providing forsakes of posterity and the knowledge of performance levels of the steel building under strong ground motions, by means of Structural Health Monitoring system, which will optimally be a contribution to the ongoing researches in this area.

1.3. Objectives of the Study

In achieving the aim of the project, the following objectives were taken.

- Gain an ability to instrument a steel building using (SHM) system
- Gain ability to obtain the dynamic properties of the building using ambient reading, recorded from the building
- The comparisons of the results obtained from the analysis of different readings
- Also to find the performance point of the building, by using nonlinear pushover analysis

1.4. Scope of the Study

- To construct a Finite Element Model of the instrumented steel building
- Select a suitable data acquisition system and instrumentation to monitor the steel building
- Instrument a steel framed building, located in highly seismic zone
- Conduct the ambient monitoring tests and download data by means of remote connection
- Post-process the data in order to extract the dynamic properties of the steel building
- Compare experimental results that were obtained at different times of a year
- Calibrate FEM to match the field measured dynamic data of the building
- Finally to draw conclusion from the results obtained

2. LITERATURE REVIEW

2.1. Seismic Instrumentation of Buildings

The main objective of seismic instrumentation program for structural systems is to improve our understanding of the behavior and potential for damage of the structures under the dynamic loads of earthquakes. As a result of this understanding, design and construction practices can be modified so that future earthquakes damage can be minimized. An instrumentation program should provide enough information to reconstruct the response of the structure in enough details to compare with the response predicted by mathematical models and those observed in laboratories, the goal here is to improve the models. In addition, the data should make it possible to explain the reasons for any damage of the structure. The nearby free-field and ground-level time history should be known in order to quantify the interaction of soil and structure. More specifically, a well instrumented structure for which a complete set of recordings has been obtained, should provide the following useful information [3].

- Check the appropriateness of the dynamic model (both lumped-mass and finite element) in the elastic range
- Determine the importance of nonlinear behavior on the overall and local response of the structure
- Follow the spreading nonlinear behavior throughout the structure as the response increase and determine the effect of this nonlinear behavior on the frequency and damping
- Correlate the damage with inelastic behavior
- Determine the ground-motion parameters that correlate well with building response damage
- Make recommendations eventually to improve seismic codes (Celebi and others, 1987)
- Facilitate decisions to retrofit/strengthen the structural system as well as securing the contents within the structures

2.2. Steps in Instrumenting a Structure

The following steps are going to be followed in order to instrument a structure [3].

2.2.1. Selection of Structure to be Instrumented

In selecting a structure for the seismic instrumentation, unless other factors are considered and/or specific organizational choices are made a priority, the following general parameters can be considered to rank structures for instrumentation:

1. Structural parameters, these include the following: - Construction Material, Structural System, Geometry of the Structure, Discontinuity and Age of a Structure.

2. Site-related parameters: - These are as follows:

- Severity-of-shaking factors to be assigned to each structure on the basis of its closeness to one or more of the main faults within the boundaries of the area considered
- Probability of a large earthquake ($M_w=6.5$ or 7) occurring on the faults within the next 30 years has to be obtained. The purpose of this parameter is to consider the regions where there is strong chance of recording useful data within an approximately useful life of a structure
- Expected value of strong shaking at the site, which is determined as the product of point 1 and point 2 above

Once the particular structure to be instrumented is identified, the engineering staff in turn obtains instrumentation permits for selected structures, gathers information related to the project including structural plans and models information, and direct structural evaluation and if necessary performs ambient response studies.

3. Requisite Information: Once it is decided to instrument a particular structure and permit is already obtained, it is imperative that a series of studies, deductions, and

decisions should be made. Furthermore, it is important to optimize the instrumentation schemes from the point of view of both cost and required data. This necessitates study of the expected dynamic behavior of the structure. The preliminary studies include the following steps:

- Study of available design and analysis information after the permission for instrumentation is granted by the owner
- Site visit, and
- Required analytical studies and tests, if feasible and necessary

In general the following information, if available, will be required:

- Relevant blueprints and design calculations
- Dynamic analysis (mode shapes and frequencies)
- If available, forced-vibration test results, and ambient-vibration test result are needed

Seldom all these information are available for any structure. In particular, for a structure that is yet to be constructed, blueprints, design calculations and if available, dynamics analyses may be all the information to design its instrumentation scheme so that part of installations of conduits and cables can be feasibly carried out during construction. The collected set of data is then used as a basis for determining transducer locations that will adequately define the response of the structure during a strong earthquake.

4. Site Visit: A general scheme can be prepared after a study of the blueprints and other available information related to dynamic characteristics. However, the general scheme for locating instruments needs to be confirmed by a site visit (for existing buildings). The structure may present various constraints that affect safe installation and reliable performance of the sensors. The site visit enables the technical personnel to make relevant changes in the prepared schemes.

5. Importance of Building Specific Free-Field Station: If physically feasible, it is advisable to include into the instrumentation scheme, a building specific free-field station. Such a free-field station is usually deployed at a distance greater than 1.5-2.0 times the height of the nearest/tallest building. This is due to the desire that motions recorded by a free-field station should not be influenced by the shaking of the buildings. As can be expected, in urban areas, this may be a problem due to the density of built facilities. In general, free-field and ground-level motions should be known in order to quantify the interaction of soil and structure. However, data recorded at building specific free-field stations can be used to urgent data bases used for structural response studies as well as ground motion studies including development of attenuation relationships and quantification of site response transfer functions and characteristics.

6. Tests on Existing Structure to Determine Its Dynamic Characteristics: Although it is possible to obtain a satisfactory understanding of a structure's expected dynamic behavior by preliminary analytical studies, when feasible and necessary, an ambient-vibration and/or a forced vibration test on an existing structure can be performed to identify mode shapes and frequencies. Ambient-vibration tests can be performed efficiently using portable recorders at three to five locations that are expected (from analytical studies or other information) to have maximum amplitudes during the first three to four vibrational modes. Thus, elastic properties of the structure can be determined. If the subjected structure experiences nonlinear behavior during a strong shaking, it will be much easier to evaluate the nonlinear behavior once linear behavior is determined before the nonlinear behavior occurs during the strong shaking.

7. Dynamic Analysis: If a dynamic analysis was not prepared by the designers of a structure or the information is unavailable, then a simplified finite-element model could be developed to obtain the elastic dynamic characteristics. This is performed with any one of the several tested computer programs available (e.g. SAP2000, ETABS and ANSYS).

2.2.2. Selection and Installation of Instruments

The selection of instruments part involves selecting the types of sensors to be used, selecting the location where the sensors should be placed, determining the number of sensors to be used, and defining the data acquisition hardware and installation process. Step one (pre-investigation of structure) play a major role in these sections.

Firstly, accelerometers, cables and data acquisition system must be chosen according to their quality and prices. The accelerometer locations should be decided based on the expected mode shapes of the structure. The number of accelerometer locations is the function of the structure size and complexity. For small and simple structures it might be just 6-12 points; however, a large number of accelerometers might be needed for large structures. After the installation of the transducers on chosen locations, and completing all the connections, set-ups of the data acquisition system must be done. By using these setups, required measurements can be taken from the data acquisition system. Figures 2.1 show several types of instruments that are used for seismic monitoring.

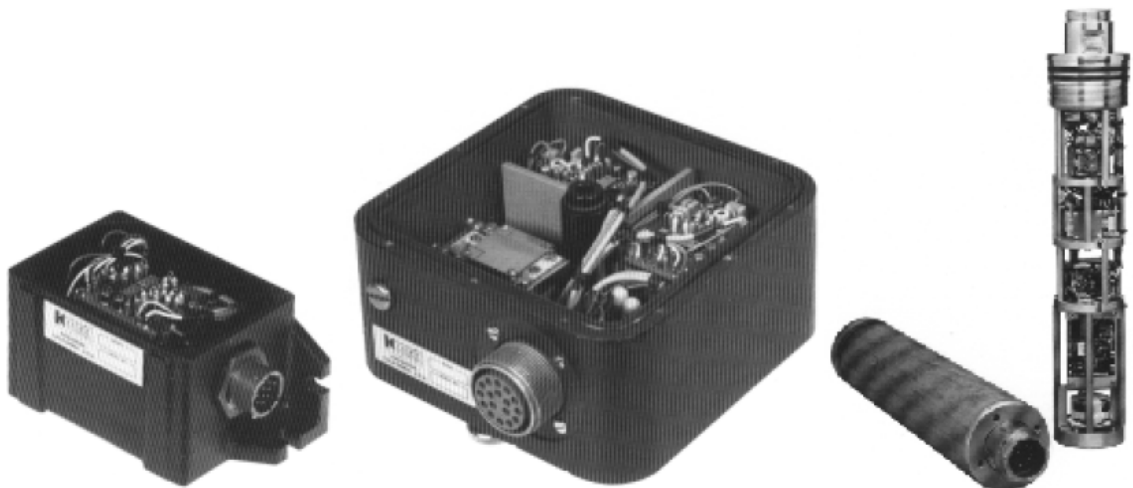


Figure 2.1. (From left to the right) Uni-axial, Tri-axial and Down-hole Forced-Balanced Accelerometers [3]



Figure 2.2. View of the force balance accelerometer (EpiSensor) [4]



Figure 2.3. View of the 24-bit strong motion accelerograph [5]



Figure 2.4. View of the geometrics 24 channel geode seismograph [6]

After the determination of instruments locations, and numbers have been obtained, the following general approach is followed to install seismic instruments:

1. After instrumentation scheme is developed and approximate sensors locations are chosen, engineers and technicians review the site to determine exact sensor locations and routing of cables and conduits. This is important from viewpoint of long-term accessibility, potential interference with the occupant's space, placement of data cable runs, and aesthetic requirements of the owner. Figure 1.5 a sample schematic diagram showing locations of sensors, routing of cables, location of junction boxes and recording units.

2. Next the engineers inspects the entire structural scheme with an electrical contractor who will install the data cable, junction boxes at key locations and terminal boxes (if required) at each sensor site.

3. The cable-termination box which includes data circuits, batteries and battery charger. This box is normally mounted on the wall above the recorder. The recorder

location is selected on the basis of security, typically in a telephone or electrical switch room, and in some circumstances is enclosed with separate fencing if it is located in an open area.

4. The instrumentation undergoes a preliminary calibration in the strong-motion laboratory and is then installed in the structure with appropriate test procedures including a static tilt sensitivity test for each component and determination of direction of motion for upward trace deflection on the record. For modern digital systems, this information is entered into the recorder data section and is stored in a general database. Other documentation includes precise sensor location, period and damping of each unit, location of cables runs, access information, and circuit diagrams.

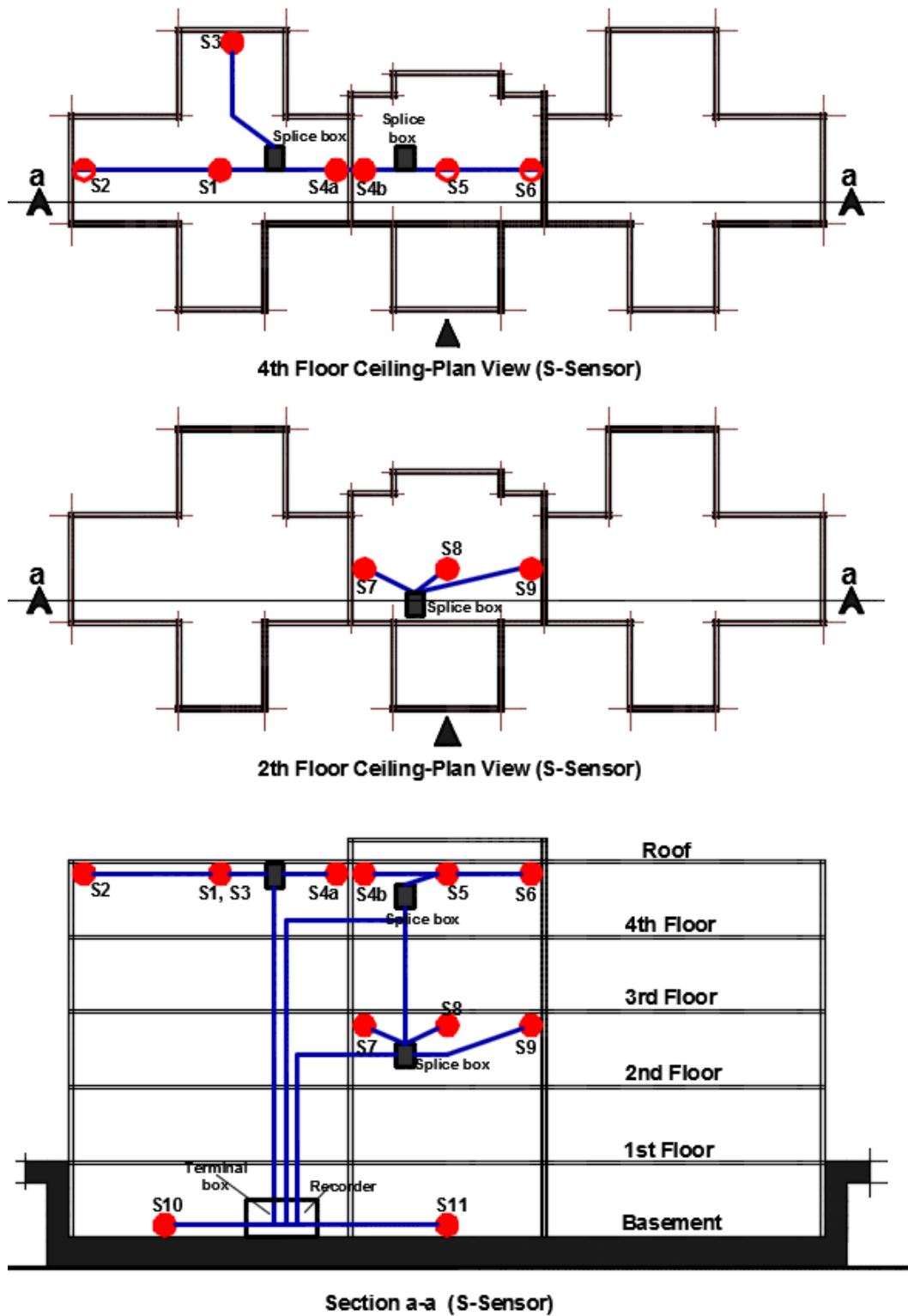


Figure 2.5. Schematic diagram showing typical deployment of sensors and routing of cables to the recorder [3]

2.2.3. Maintenance

It is essential to have periodic and consistent maintenance of instruments to have a successful program. Unless maintenance arrangements are made, successful recording of data cannot be accomplished. Therefore, routine maintenance is conducted every 3-12 months if circumstances and experience so allow. This maintenance includes the following:

- Remote calibration of period and damping
- Inspection of battery terminals, load voltage, and charge rate (batteries are replaced every 3 years)
- Measurement of threshold of triggering system and length of recording cycle. As a final maintenance procedure, a calibration record is obtained and then examined for the desired characteristics

2.2.4. Testing, Measurement, and Post Processing of Recorded Data

The dynamics response measurements, which are received from the data acquisition system, are recorded by using simplistic data acquisition software. Stored measurement files are translated into suitable file formats for the subsequent processing steps.

The recorded and translated data records are analyzed in commercially available software to obtain the experimental modal parameters. These experimental modal parameters can be verified by using different sets of measurements which are taken in different times of a year. Furthermore, the quality of the measurement can also be investigated by using different experimental testing techniques together such as forced vibration testing and ambient vibration testing. This study gives an engineer a chance to control the reliability of experiments.

Another option is that different estimation techniques of one vibration measurement type can be used to analyze post-processing reliability of the recorded data for

the same time interval. Using different estimation techniques can be repeated several times for different time intervals.

2.2.5. Comparison Against FEM and Evaluation

The last but not the list, here the behavior of a structure under various types of loadings is simulated by Finite Element Analysis (FEA). Finite Element Analysis refers to the predictive approach that relies on the quality of the following (simulation model, software to analyze it, and approach that relies on the quality of the analyst interpreting the results). Several assumptions are made by engineers when the finite element model of the structure is created in any computer software. These assumptions and the reliability of the finite element model can be controlled in light of the output of the recorded data from the structure. Here the experimental study provides a comparison between the real structure and the computer model of the structure.

With the comparison, if necessary, calibration of the finite element model can be done. Calibration or Model Updating is carried out by modifying the mass, stiffness, support conditions, and damping parameters of the FE model until an improved agreement between finite element analysis data and the tested data is achieved. For that comparison, required true modal parameters are natural frequency (resonance frequency), mode shapes (that is the way the structure moves at certain resonance frequency), static loading test results, and damping ratio. Static loading test may not be available for buildings and are mostly common to bridges. Modal parameters are important because they describe the dynamic properties of a structure. They constitute unique information that can be used for model validation and model updating.

The conclusion part of the experimental study (Structural Health Monitoring) will provides enough information about the reliability of the structure's finite element model. A comparison between the true modal parameters, obtained from the recorded data and the modal parameters of the structure's finite element model is made. Here, if the analysis shows more divergence between the true model and finite element model of the structure, then there exist two options.

- First one states that the finite element model of the structure is not dependable and calibration works are required
- Second option is that structure may be damaged because of any environmental affects

The divergence can also occur due to wrong assumptions which were made by the engineers during the modeling, wrong information about material property, about structural system, support conditions, geometrical dimensions and or mass of the structure. Both results require starting a new study on the structure, which is either calibration of the analytical model or the strengthening of the structure.

2.3. Previous Studies on Structural Health Monitoring and Performance Analysis

For the past several decades, the Structural Health Monitoring for buildings, dams, elevated railways, and skyways were not given much attention. Many buildings and other infrastrucutres mentioned above have not installed or operational Seismic Monitoring Instruments intended to continuously monitor their strucutral health and integrity. Without these instruments, no monitoring records can be presented to determine the integrity and serviceability of the building before, during, and most especially in an aftermath of a major Earthquake [7]. Today, the modern world is moving ahead for an advance and comprehensive SHM technological trend to monitor the state of a structure during service. Below are the several studies that took places on Structural Health Monitoring and performance analysis.

Following the 27 February 2010 ($M_w = 8.8$) Offshore Maule, Chile earthquake, a temporary, 16-channel, real-time data streaming array was installed in a recently-constructed building in Vina del Mar to capture its responses to aftershocks. The cast-instu, reinforced concrete building is 16 stories high with three additional basement levels, and has dual system comprising multiple strucutral walls and perimeter frames. This building was not damaged during the main-shock, but other buildings of similar design in Vina del Mar and other parts of Chile were damaged, although

none collapsed. The building was chosen in order to understand the dynamic characteristics of a dual system (core structural wall and perimeter moment frame-wall) building which is a typical construction found in Chile. This types of construction, in general, performed well during both the M7.8 Valparaiso earthquake in 1985 and the recent Maule event. Located approximately one block away from the Vina del Mar Centro strong motion station that recorded peak acceleration of 0.33g [8]. In this study Spectral Analyses (Bendat and Piersol, 1980) were used to extract the significant frequencies. In addition, system identification techniques were used extensively to extract similar dynamic characteristics. The result shows that dual core systems which comprise core structural wall and perimeter-wall perform well during strong shaking.

A state-of-the-art seismic monitoring system comprising 36 accelerometers and a data-logger with real-time capability was installed at Building 54 on the Massachusetts Institute of Technology (MIT), Cambridge, MA campus. The system is designed to record translational, torsional and rocking motions, and to facilitate computation of drift between selected pairs of floors. The cast-in-situ reinforced concrete building is rectangular in plan but has vertical irregularities. Heavy equipment is installed asymmetrically on the roof. Spectral analyses and system identification performed on five sets of low-amplitude ambient data reveal distinct and repeatable fundamental translational frequencies in the structural NS and EW directions (0.75 and 0.68Hz, respectively), a torsional frequency of 1.49Hz, a rocking frequency of 0.75Hz, and very low damping. Such results from low-amplitude data serve as baseline against which to compare the behavior and performance of the building during stronger shaking caused by future earthquakes in the region [9].

A 64-story, performance-based design building with reinforced concrete core shear walls and unique dynamic response modification features (tuned liquid sloshing dampers and buckling-restrained braces) has been instrumented with a monitoring array of 72 channels of accelerometers. The responses of the building to ambient motions from ground or wind were recorded and analyzed to identify modes and associated frequencies and damping. Not unexpectedly, the low-amplitude dynamic characteristics are considerably different than those computed from design analyses. Nonetheless, these

computed values serve as a baseline against which to compare future strong shaking responses. Such studies help to improve our understanding of the effectiveness of the response modification features at various levels of shaking, to evaluate the predictive capabilities of the design analysis tools and to improve similar designs in the future [10].

In 1996 a study of performance analysis of steel building was taken place [11]. Due to January 17, 1994 Northridge Earthquake, the building is 11-story moment-frame. During the field investigations virtually all the frame connections in the building were exposed and visually inspected. The building consist of six levels office spaces over five parking levels. The approximate footprint of the building (plan dimensions of the parking levels) is 90 feet width in (N-S direction) and 260 feet long in (E-W direction). The office level plan dimensions vary from 145 feet wide by 205 feet long at the roof level to 190 feet by 260 feet at the first office floor.

The building is constructed of composite concrete and steel deck slabs which are supported by A36 structural steel beams and columns. The exterior skin is made of precast concrete panels and glass plates. Structural steel columns are supported at the foundation by cast-in-place reinforced concrete friction piles. The seismic loads resisting system appears to consist of ordinary moment frames constructed of A36 structural steel girders and columns. These systems are called (Ordinary moment frames) this is because in many cases they do not satisfy today's strong column-weak girder design provisions and the continuity/double plate requirements.

There is a 260 feet long two story reinforced masonry shear wall at the south side of the structure which also serves as a lateral load resisting element. Seismic loads are delivered to the lateral resisting elements by the composite concrete and steel deck slabs which act as horizontal diaphragms. Seismic loads in the lateral system are resisted at the foundations by the cast-in-place friction piles, and soil friction below the concrete slab-on-grade. A three-dimensional computer model of the building was generated using the ETABS computer program, the elastic demand/capacity ratios (DCR) were calculated using LRFD formulations. Elastic (DCR) values suggest that for the synthetic motion postulated for the site of the building should have remained

essentially elastic. Two nonlinear 2-D computer models were also constructed (one for the E-W and the other N-S direction). In each computer model, all frames in the direction under consideration were included and connected by the rigid floor diaphragm assumption. Bilinear hysteric behavior was assumed using a 5The results obtained from the performance analysis of the 11-story steel moment framed building revealed the following:

- The damage observed was much more extensive than that predicted by the analyses
- The average beam DRC at damaged connection is 20
- Elastic beam stresses correlate better than other analytical indicators with the severity of the observed damages, the inelastic column damage index is the second best
- Both elastic and inelastic analyses indicate that the columns are relatively weaker than beams and the nature and extent of observed damage correlates this trait
- The results of the nonlinear pushover analyses correlate relatively well with results obtained by inelastic dynamic analyses for ground motions various severity

3. EXPERIMENTAL STUDY AND DATA ANALYSIS

3.1. Introduction

Seismic instrumentation of building is intended for Structural Health Monitoring, which refers to the process of implementing a damage detection and characterization strategy for engineering structures. In various countries around the world including Turkey being prone to major earthquake disturbances, there has been an increasing concern on the SHM technology consisting of digital data acquisition system being integrated to the internet data transferring network.

Several decades ago, it was recorded by various government earthquake monitoring agencies and engineers around the world that many buildings and infrastructures were damaged and others collapsed due to Major Earthquake. Other buildings and infrastructures survived but sustained minor to severe structural concrete cracks and physical deformations [7]. Due to these earthquake scenarios, the need for SHM becomes very essential requirements and utmost attention for SHM becomes decisive.

3.2. Selection of Structure to be Instrumented

Structural Health Monitoring was applied to the six-story steel hinged-framed building with one additional basement floor (Figure 3.1) located in Hatay Antakya, it was built in 2009. Antakya is located in the first earthquake region in Turkey. The Soil type of the building is (Z2) according to the information from the building design project. The building is rectangular in shape (29.5m by 20.5m), the basement floor is 3.6m while the typical floors are 3m heights, with a total height of 24.6m from the base. During the construction the steel members (HE300A and HE240A) for columns, (IPE200, IPE270, IPE300, IPE400 and IPE450) for the beams are used. The thickness of the concrete slabs for all floors is 150mm; all the stories have the same plan except for the ground-floor and the six-floor as shown in Figures 3.4. to 3.6.

The lateral force resisting system of the building is a dual system, which comprises of two central core reinforced concrete (R/C) walls, and steel frames. The joint for the steel beams to the column is hinged connection, Figure 3.1. is showing the instrumented steel building.



Figure 3.1. Six-story steel hinged-framed building

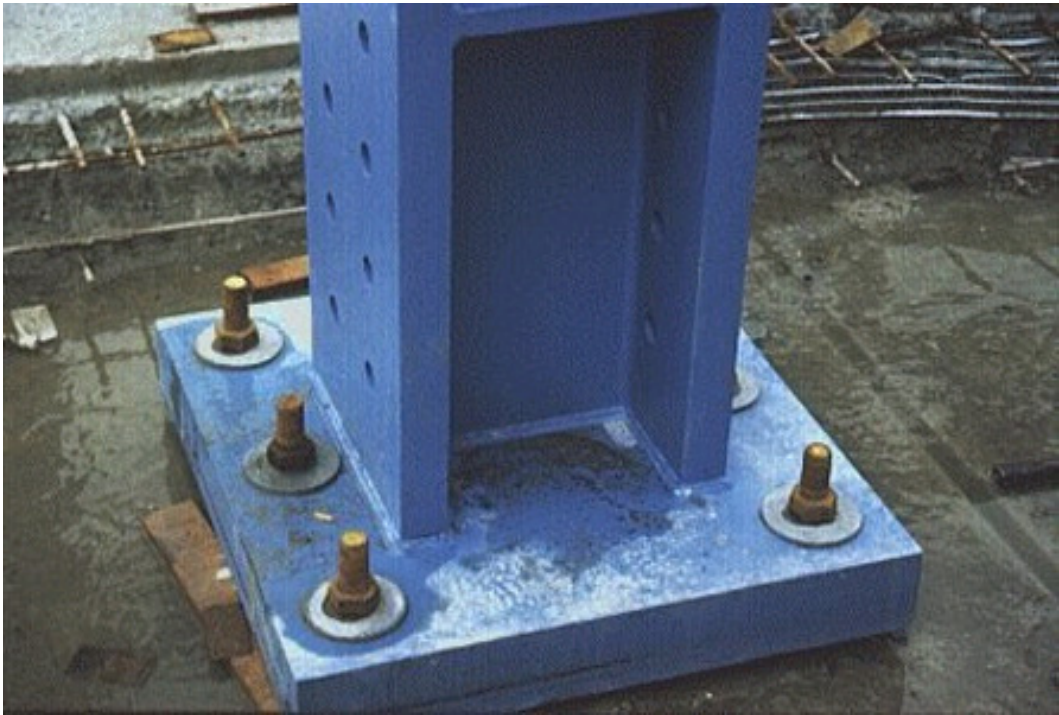


Figure 3.2. Foundation connection (Rigid connection)

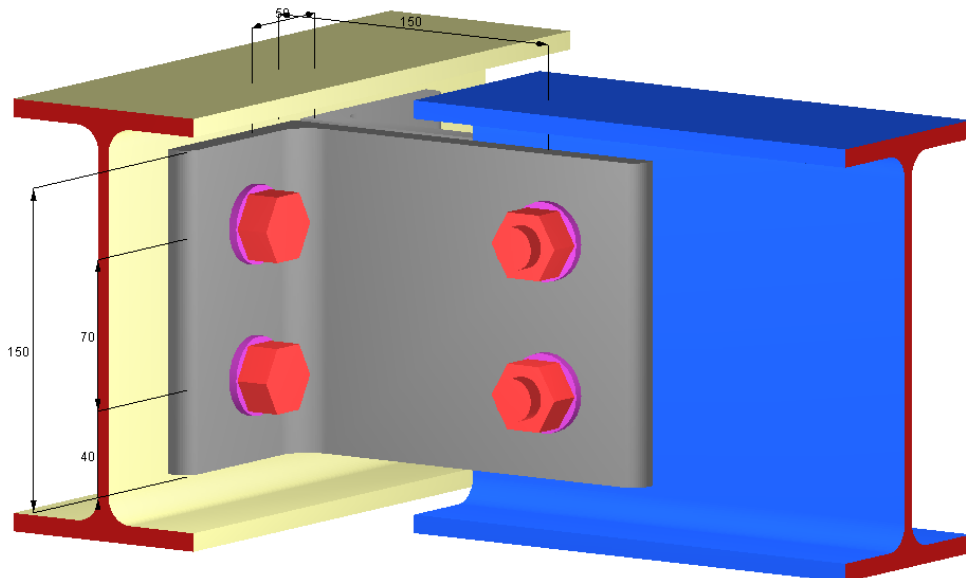


Figure 3.3. Beam to beam hinge connection [12]

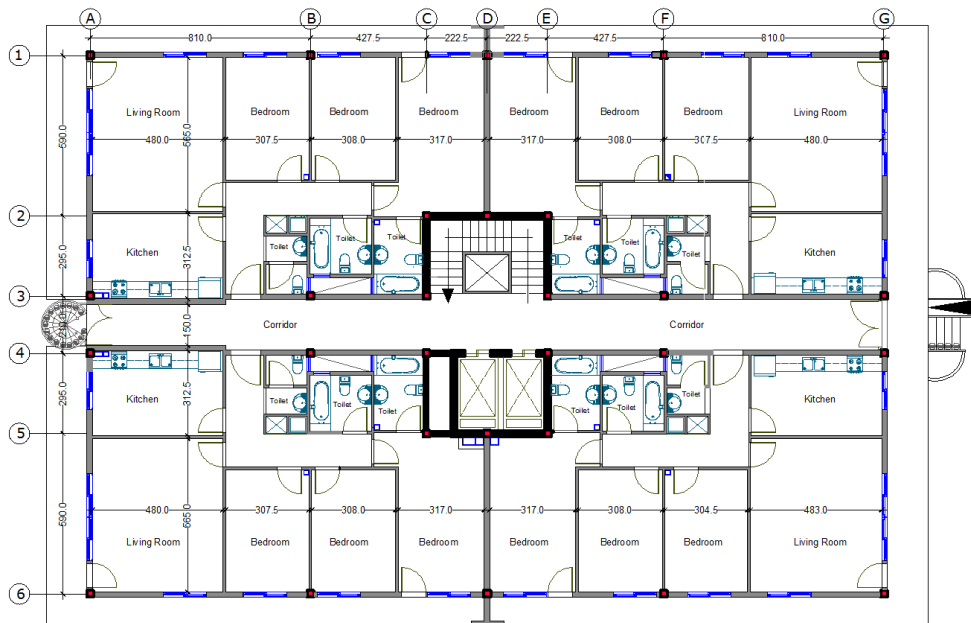


Figure 3.4. Ground floor plan view showing the distribution of steel columns and central shear walls

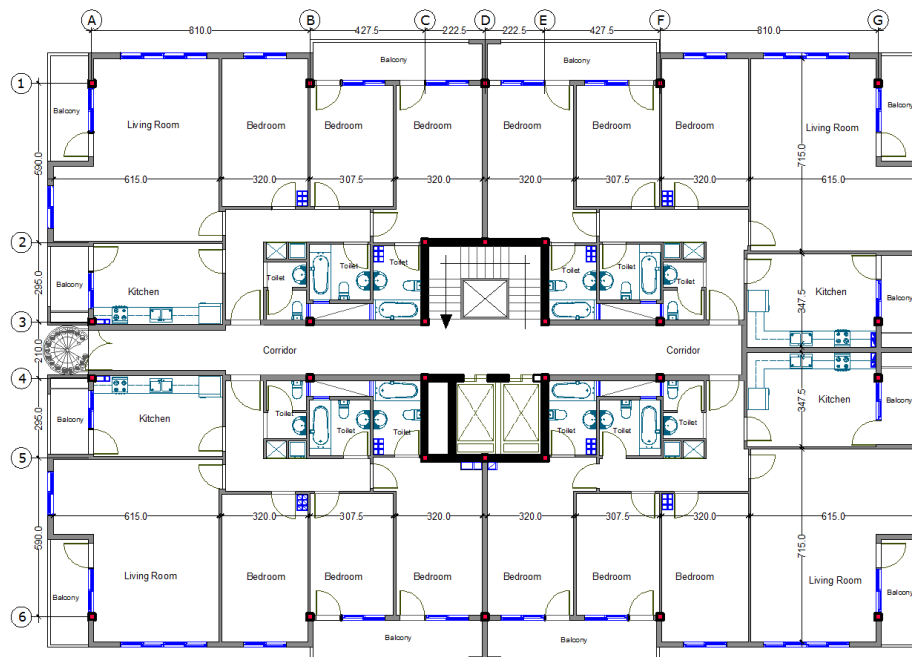


Figure 3.5. Typical (1st to 5th) floors of the building, showing the distribution of steel columns and central shear walls

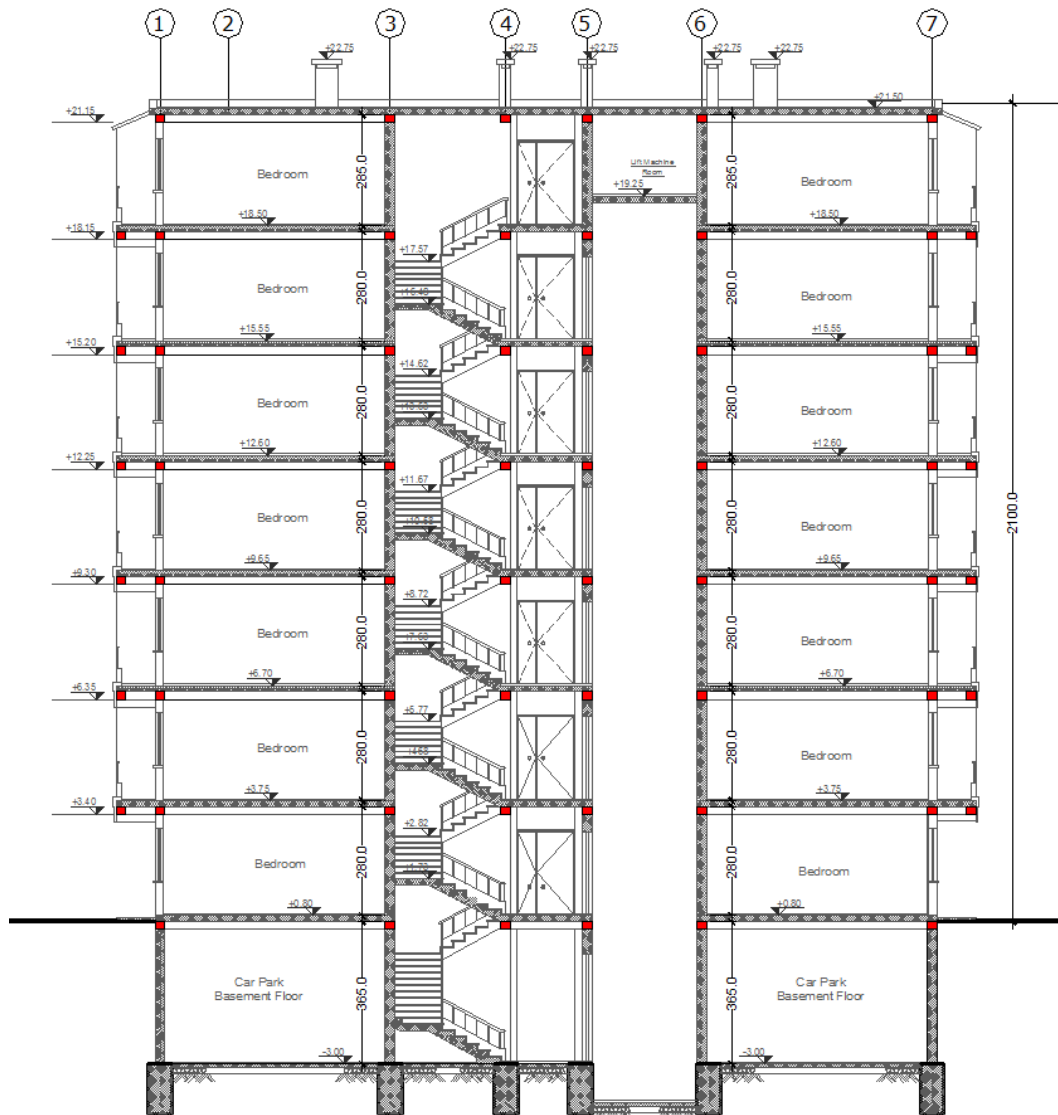


Figure 3.6. Section cutting through the building, showing the distribution of steel columns, beams as well as the central core shear wall

The probable magnitude of Earthquake expected in Antakya is (Mw 7.0) according to some researchers, with the reference of the (Mw 5.8) of January-22 1997 [13]. And the faults within the boundaries of the area considered as shown in Figure 3.7.

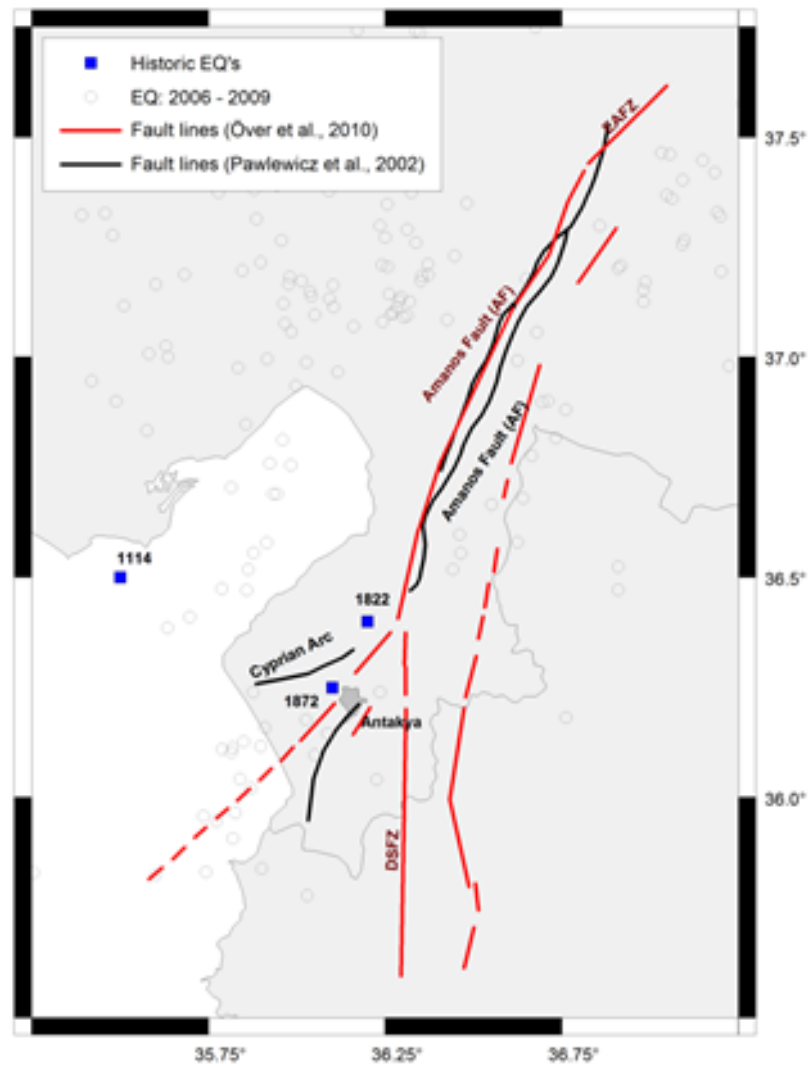


Figure 3.7. Earthquake faults region [13]

The building free-field station is located away from the main building; because the motions recorded by a free-field station will not be influenced by the shaking of the building. In general, free-field and ground-level motions should be known in order to quantify the interaction of soil and structure [3]. However, data recorded at building specific free-field stations can be used for structural response studies as well as ground motion studies including development of attenuation relationships and quantification of site response transfer functions and characteristics. Figure 3.8. Shows the location of the building free-field.



Figure 3.8. Showing the building-free located away from the main building

The building free-field contains three sensors, which are used to record three movements the first two in horizontal (X and Y) directions and the third one in vertical (Z) direction.

3.3. Selection and Installation of Instruments

The selection of instruments part involves selecting the types of sensors to be used, selecting the location where the sensors should be placed, determining the number of

sensors to be used, and defining the data acquisition hardware and installation process. Below are the descriptions of the instruments used in acquiring the data from the instrumented building.

3.3.1. Strong Motion Accelerometer

The type of the strong motion accelerometer used in this project is CMG-5U Figure 3.9. This is single-axis strong-motion force feedback accelerometer in a sealed case. This accelerometer is used either in vertical or horizontal orientations according to CMG-5U manual.



Figure 3.9. CMG-5U Strong motion accelerometer

Strong-motion accelerometers were designed to record the strongest events, that is when the ground motion reaches the level where humans can feel it, typically (1-2 percent g) and the weak-motion accelerometers were designed to record very weak events [14]. Therefore CMG-5U has been used as the strong-motion accelerometer in order to capture the responses of the building.

Acceleration is measured in ‘g’, where 1g corresponds to the vertical acceleration force due to gravity. During an earthquake, the forces vary a lot and keep changing. The largest earthquake forces that have been measured are about (1 to 2g) most earthquakes have much lower forces [14]. Full-scale low-gain sensitivity of 5U sensors is available from 4.0g down to 0.1g and the high gain sensitivity of 5U sensor is available from 0.4g to 0.01g (CMG-5U manual) level range determines the maximum g load a device can measure accurately. It can also indicate the maximum acceleration that a device can withstand without damage or permanent scale shift. It should be noted that the maximum acceleration encountered can be substantially higher than expected, because of the incorrect mounting or loose parts (CMG-5U manual).

In this project 12 CMG-5U Strong-Motion Accelerometers were used to obtain the responses of the building: three in the second-floor, three in the fourth-floor, three in the six-floor and the remaining three in the free-field station.

3.3.2. Data Acquisition System

In this project CMG-DM24S12AMS data acquisition were used to obtain the responses of the building Figure 3.10.



Figure 3.10. Data acquisition system, located in the cabinet for safety

CMG-DM24S12AMS data acquisition system is a self-contained seismic data collection station configured to operate 12 single-component strong-motion accelerometers (CMG-DM24S12AMS manual). The sockets of these twelve accelerometers are placed at the back side of the data logger. Other six sockets are placed at the front side of the data logger (Figure 3.10) for digital output seismometers. In addition to these six digital seismometers, auxiliary inputs are placed on the front side of the data logger system. Power can be supplied to the sensors by these sockets. At the right part of the front side, there are also other six sockets: one for telephone, one for network cable, one for GPS cable, one for USB connection, and the other for power sources. Also Figure 3.10. shows how an integrated laptop PC is combined by the data logger system for viewing and transmitting the recorded data, Appendix A. Scream software is been loaded to the laptop PC, therefore all the setup and control of the recorded data are provided by the Scream software. Twelve number of strong-motion accelerometers were connected to the data logger which was placed in the steel building located in Antakya (Hatay). All the data recorded by the instruments is fed into the data logger (DM24S12AMS), where it can be stored and then later download from our main system using Team Viewer Software via internet connection.

The data acquisition system (DM24S12AMS) can be powered either from 110-120V AC mains power, or from a 12V DC power source. But, whenever there is power failure to the system all the setups and the data logger are going to be lost, so in order to prevent this kind of failure, in addition to the methods mentioned above a BATTERY/UPS is been connected to the system in order to prevent the system from power failure.

The CMG-GPS2 is used as the GPS system in the project; the system is a stand-alone unit requiring only one cable connection to the DM24S12AMS, which carries both signals and power. The function of GPS is to provide time synchronization according to the Greenwich Mean Time. Maintaining a good fix from the available satellites which is the most important point about the GPS. If that situation is provided exactly the system will then switch on the control process and set the internal clock. Otherwise, a discontinuity occurs in the data, during recording.

3.3.3. Scream Software

Scream software is the main brain of the data acquisition system, all the controls of the sensors, recording and triggering options are provided by the software. By using the software the option listed below can be controlled.

- The type of sensors
- GPS power cycling options
- The short-term and long-term average values for triggering
- The length of free-trigger and post-trigger periods
- Calibration signal inputs
- Length of the recorded data
- Frequency of the continuous and trigger readings
- Transmitting data

In the configuration Setup Window of the software it provides a GPS options. GPS unit receive time signals constantly, and that give the most accurate results with ample power during the recording. But when there is power failure in the system, there is another option provided to the GPS. In that option, the GPS time is only checked at the intervals of a specified number of hours. Where any whole number of hours can be chosen for the interval. But in this project power is been provided to the system constantly, therefore the GPS receive time signal constantly.

In the scream software the incoming data is internally sampled at 2000Hz. After filtering and reducing that data to a lower rate, the system (DM24S12AMS) record data continuously at a relatively sample rate and record at a much higher sample rate during short periods when the trigger is active (DM24S12AMS manual). In this thesis, continuous readings were recorded at 100Hz and triggering reading was recorded at 200Hz.

In the Scream software two trigger options exist. One is STA/LTA Triggering and the other is LEVEL Triggering. The STA/LTA algorithm applies a simple short term

average calculation to the triggering stream. That calculation is based on the ratio of the STA/LTA algorithm. When the ratio of the averages exceeds the chosen ratio value an event is usually present and data starts being recorded in a file. In this way record of the noise data will be prevented. These ratios can be given to the Scream for each channel to determine a trigger. But, the important point is that STA/LTA ratios of the all chosen channels must be the same. If any of the chosen channels passes the trigger condition, the trigger will activate and will not de-trigger until all of the chosen channels have fallen below their respective ratio values (DM24S12AMS manual).

Short term averages and long term averages are calculated in time intervals. Typically, the time interval of the short term average should be about as long as the signals wanted to be trigger on and the time interval of the long term average should be taken over a much longer interval. These time intervals were chosen as 1 second for STA and as 10 seconds for LTA. It means that Scream determines the maximum recorded values as STA for every 1 second and the maximum recorded value as LTA for every 10 seconds. If the ratio between these maximum values of STA and LTA exceeds the given ratio which was 4 in this project, system process the trigger condition. Both the STA and LTA values are recalculated continually, even during a trigger. In the trigger condition, Scream starts to record trigger readings during pre-trigger and post-trigger time intervals for every channel.

All the recorded data are stored on the local hard disk. Scream controls the way of storing the data, according to the setups specified. The total size of the laptop's 'C' drive is 15.7 GB. To use its hard-disk space effectively, two options are provided by the software.

- One is “Stop when Disk Full”. If this option is selected, Scream will stop the recording when the disk is full
- The second one “Ring Buffer”. If this option is selected, Scream will start deleting the oldest data in the directory of the computer in order to make space for new recorded data, so the most recent recorded measurements are always protected.

Also recorded readings can be seen in GCF format, as a graph without converting the file by using Scream (Figure 3.11). While Figure 3.12. is shown the recording channels of the data acquisition system.

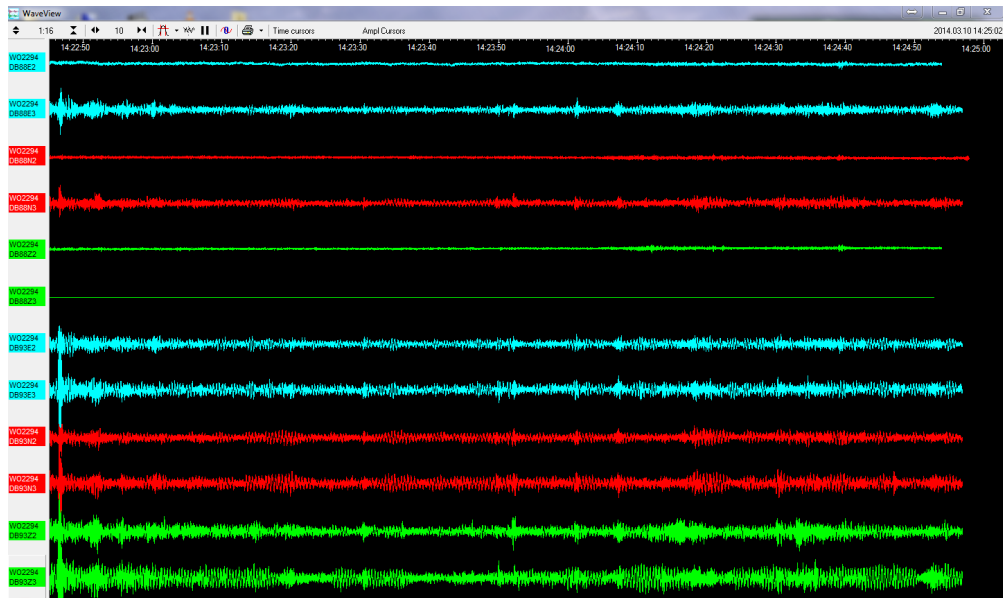


Figure 3.11. Graphical view of 12 recording channels data, using Scream Software

Stream ID	Rec.	Comp.	SPS	End Time	Date	RIC
DB93Z3	Yes	16 bit	100	14:03:40	11.02.2014	-2820883
DB93Z2	Yes	16 bit	100	14:03:41	11.02.2014	-2699052
DB93N3	Yes	16 bit	100	14:03:43	11.02.2014	-2894449
DB93N2	Yes	16 bit	100	14:03:39	11.02.2014	-2904464
DB93E3	Yes	16 bit	100	14:03:43	11.02.2014	-2847710
DB93E2	Yes	16 bit	100	14:03:43	11.02.2014	-73892
DB9300	Yes	8 bit	0	14:01:00	11.02.2014	N/A
DB88Z3	Yes	8 bit	100	14:03:42	11.02.2014	-583945
DB88Z2	Yes	8 bit	100	14:03:36	11.02.2014	-1086792
DB88N3	Yes	16 bit	100	14:03:43	11.02.2014	-3407069
DB88N2	Yes	16 bit	100	14:03:34	11.02.2014	-617225
DB88E3	Yes	16 bit	100	14:03:40	11.02.2014	-522309
DB88E2	Yes	8 bit	100	14:03:35	11.02.2014	-2330894
13 streams		2,056 Kb stream buffer		PC Time (UTC): 13:52:53		

Figure 3.12. View of the (12 recording channels) in Scream Software

3.3.4. Installation Process

The accelerometers are located in X Y directions of the stories to capture the dominant responses of the building in both directions. X-direction is selected to be parallel to the road in front of the building while the Y-direction is perpendicular to the road axis. For the free-field station three accelerometers were selected and the GPS antenna was located at the roof level. The location of the accelerometers can be seen in the Figure 3.13.

After the installation of all instruments, then all the cables coming from the 12 accelerometers was connected to the data acquisition system in the building and the necessary configurations was made in the Scream software, and the internet connections was obtained from the data acquisition system and our local computer.

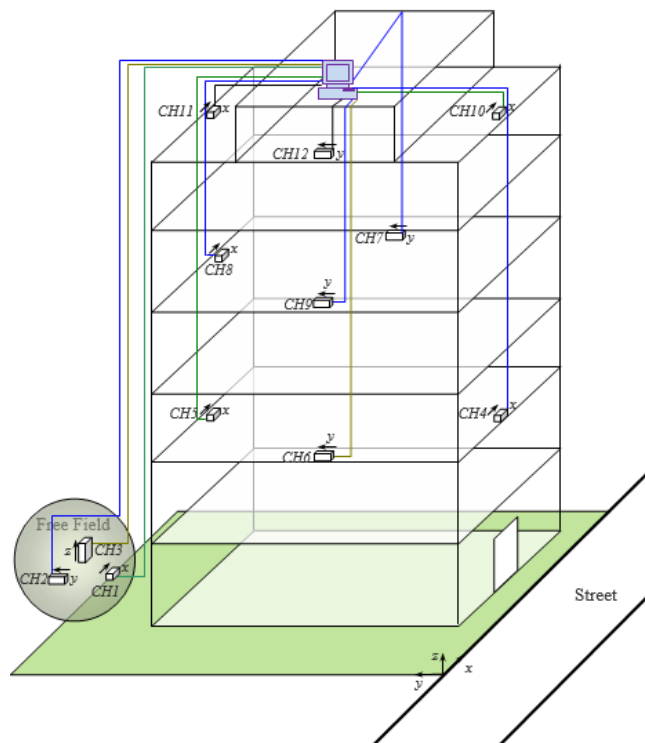


Figure 3.13. Schematic view of the building depicting location as well as the orientation of the 12 accelerometers in the building and free-field (The arrows indicating the orientation of positive acceleration for each sensors)

3.4. Post Processing of the Recorded Data

During the monitoring of the building several responses were recorded and transmitted via internet to the authors. In this thesis three sets of data were selected from the several records and used to find the response of the building, one of the reading is a moderate earthquake with a magnitude of ($M_w = 4.5$) Figure 3.14 [15]. While the remaining readings were an ambient data, as shown in the Table 3.1.

Table 3.1. Summary of the ambient/earthquake data recorded from the building

Event Type	Event Date	Origin Time, UTC	Local Time	Lat /Long	Mw	Depth (km)	Approx. Dist. From Building
Ambient	Nov 11, 2013						
Earthquake	Feb 14, 2014	00:33	02:33	36.725N/ 36.020E	4.5	17.1	65(km)
Ambient	March 1, 2014						

Some signal processing was performed on the recorded raw data in order to transform them for final use. To extract the frequency contents of signals, and remove the high frequency noise components present in the signals. A self-executable program (GCF2ASC.EXE) Produced by Guralp systems was used to convert the data to (ASCII) format from (GCF) format. The first signal processing to perform on the measured data is the Baseline Correction. The purpose of Baseline Correction is to allow us to flatten the baseline of our data and make it equal to zero.

After Baseline Correction, Filtering was applied to the data, the aim here is to shape the signal in the frequency domain. In the SeismoSignal software Lowpass, Highpass, Bandpass and Bandstop filter types are available. These type of filter options

are helpful in order to investigate the data on different frequency ranges. For this thesis Bandpass filter was selected for the filtering option. For the Signal Processing SeismoSignal and MATLAB R2008a software are used.

A program is prepared in MATLAB to process the data by using Fourier analysis. The graphical interface of the program is shown in the Figure 3.15.

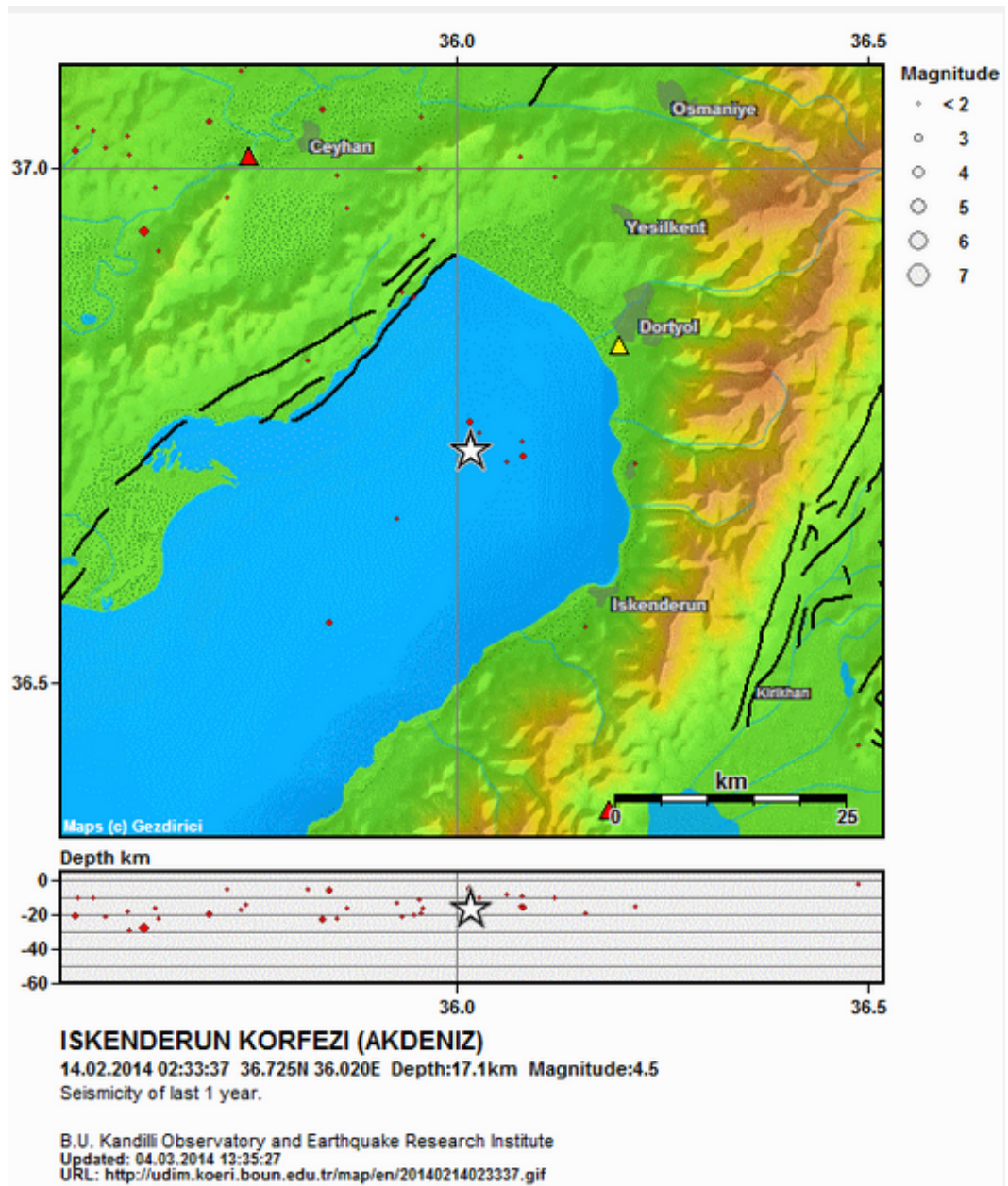


Figure 3.14. Location of the recorded earthquake, Feb 14, 2014 at 02:33am [15]

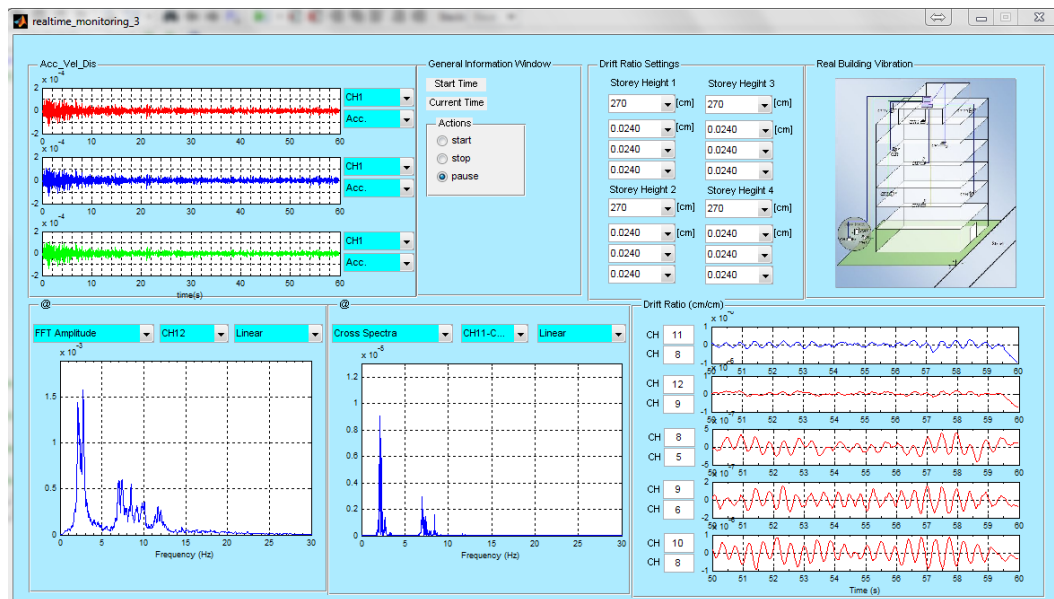


Figure 3.15. Graphical User Interface (GUI) of the program writing in MATLAB, for Data Processing in Real-Time

3.4.1. Fourier Analysis

Fourier analysis is performed to extract the frequency content of signals. For this purpose, the Fast Fourier Transform (FFT) algorithm is utilized.

3.4.2. Fast Fourier Transform

The Fast Fourier Transform is a widely-used method of extracting useful information from sampled signals [16]. The Fourier Transform is a main mathematical procedure that transforms a function from the time domain to the frequency domain. It operates on continuous functions, defined at all values (t). However, digital signal processing involves discrete signals sampled at regular intervals of time rather than continuous signals. The Discrete Fourier Transform (DFT), a modified form of the Fourier Transform, is used for sampled signals.

The sine and cosine coefficient determined by the (DFT) represent the amplitudes

of each of the frequency components of the original signal. However, the (DFT) requires a great computation time. For this reason, an algorithm developed by Cooley and Tukey [17], named as the Fast Fourier Transform (FFT), which reduces the required computation time considerably, is used to perform DFT on sampled signals [18].

For a continuous function of one variable $f(t)$, the Fourier Transform $F(f)$ is defined as:

$$F(f) = \int_{-\infty}^{\infty} f(t) \cdot e^{-j2\pi ft} dt \quad (3.1)$$

And the inverse transform as

$$F(f) = \int_{-\infty}^{\infty} f(t) \cdot e^{j2\pi ft} dt \quad (3.2)$$

Where (j) is $\sqrt{-1}$ and e use to denotes the natural exponent

$$e^{j\theta} = \cos \theta + j \cdot \sin \theta \quad (3.3)$$

Consider a complex series $x(k)$ with N samples of the form

$$x_0, x_1, x_2, x_3 \dots x_{N-1} \quad (3.4)$$

Where (x) is a complex number

$$x_i = x_{real} + j \cdot x_{imag} \quad (3.5)$$

Further, assume that the series outside the range 0, N-1 is extended N-periodic, that is $x_k = x_{k+N}$ for all k. The FT of this will be denoted as $X(k)$, it will also have N samples. The forward is defined as, For $n=0 \dots N-1$

$$X(n) = \frac{1}{N} \sum_{k=0}^{N-1} x(k) e^{-jk2n/N} \quad (3.6)$$

The inverse transform is defined as, for $n=0 \dots N-1$

$$X(n) = \frac{1}{N} \sum_{k=0}^{N-1} x(k) e^{jk2n/N} \quad (3.7)$$

Although the functions here are described as complex series, real valued series can be represented by setting the imaginary part to 0. In general, the transform into the frequency domain will be a complex valued function, that is, with magnitude and phase.

$$Magnitude = \|X(n)\| = \sqrt{x_{real} * x_{real} + x_{imag} * x_{imag}} \quad (3.8)$$

$$phase = \tan^{-1} \left(\frac{x_{imag}}{x_{real}} \right) \quad (3.9)$$

3.4.3. FFT Application on the Recorded Data

Fast Fourier Transform is carried out to examine the frequency of the recorded data. The results will be used in evaluating the period of the building. Also allows an assessment of actual dynamic characteristics and significant modal behaviors that may not always be identified or accurately determined by modal analyses with mathematical models [8].

3.4.4. Analysis of Ambient Data Recorded on (Nov. 11, 2013)

The ambient data recorded on Nov. 11, 2013 was processed and analyzed in MATLAB by using Real-Time monitoring program, have been written based on the Fast Fourier Transform (FFT). Figures 3.16-18 show the plots of the Displacement of the building obtained by double integration of the acceleration records which were given in Figure 3.11.

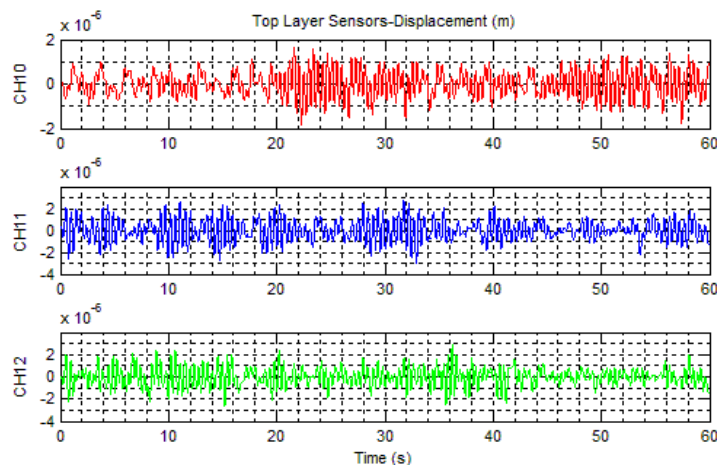


Figure 3.16. Displacement plot of the top three sensors (Top Layer) in meters

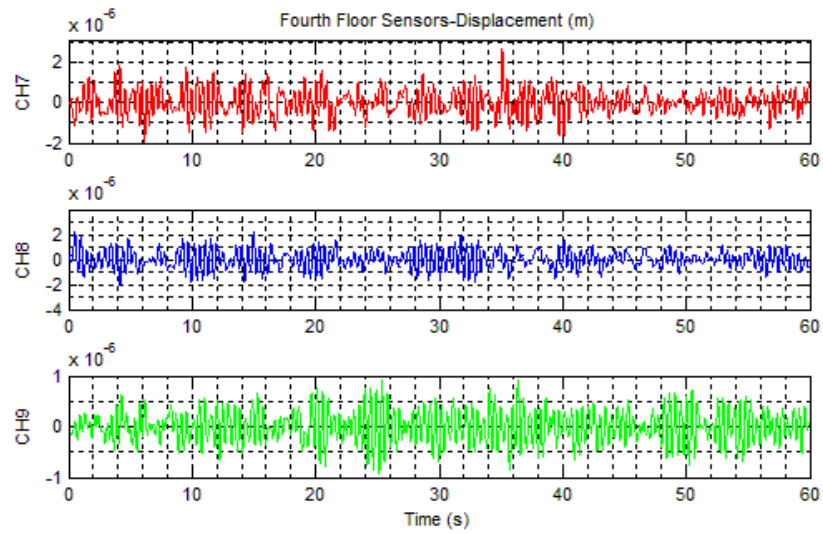


Figure 3.17. Displacement plot of the three sensors in the fourth floor, in meters

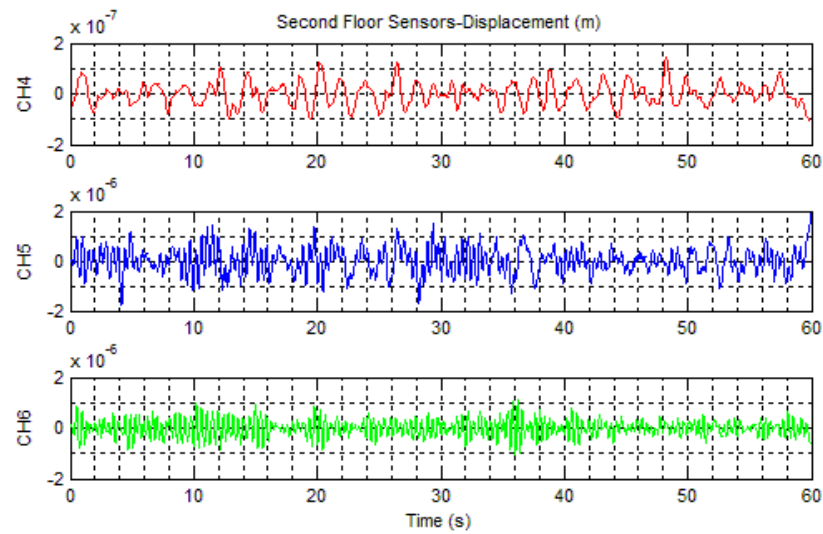


Figure 3.18. Displacement plot of the three sensors in second the second floor, in meters

Figures 3.19-21 shows the Fourier Amplitude plots of all the 9-channels in the building.

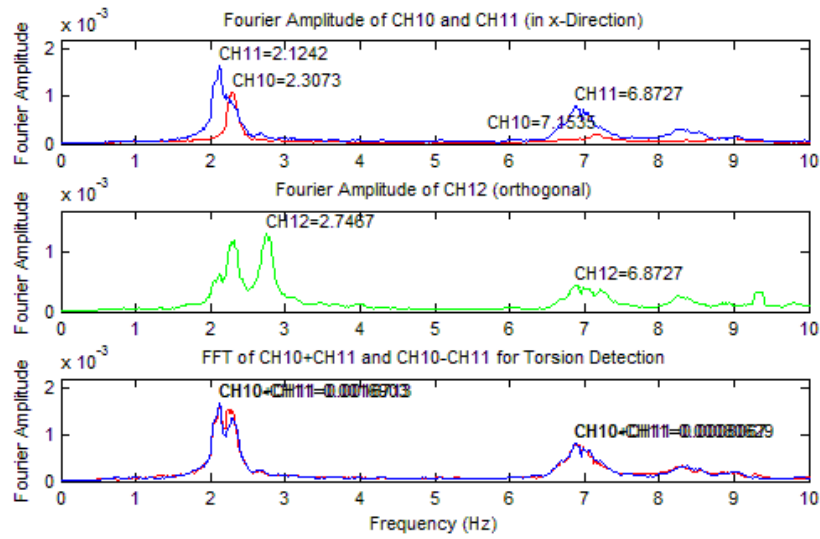


Figure 3.19. Fourier Amplitude plot of the top sensors, sixth floor (x-direction). The first plot is CH10 and CH11, the second plot is CH12. The third plot is $(CH10+CH11)$ and $(CH10-CH11)$ for torsion detection in the building

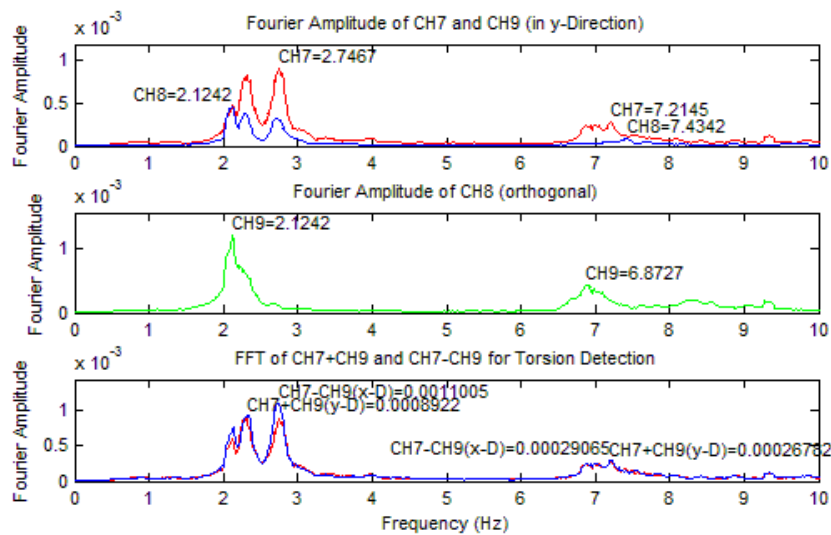


Figure 3.20. Fourier Amplitude plot of the sensors in fourth floor (y-direction). The first plot is CH7 and CH9, the second plot is CH8. The third plot is $(CH7+CH9)$ and $(CH7-CH9)$ for torsion detection in the building

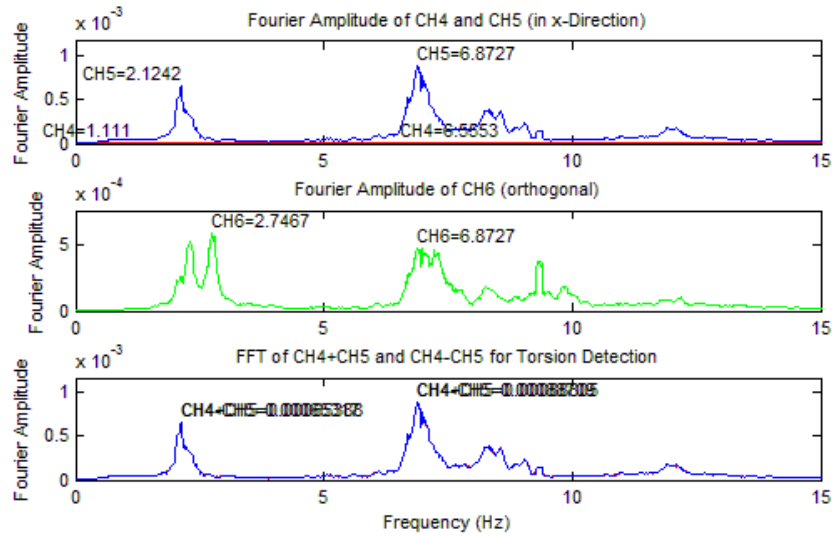


Figure 3.21. Fourier Amplitude plot of the sensors in second floor (x-direction). The first plot is CH4 and CH5, the second plot is CH6. The third plot is (CH4+CH5) and (CH4–CH5) for torsion detection in the building

Table 3.2. Summary of the experimental results obtained from the building, using ambient data

Event Type	Event Date	Channel	1st (f)Hz	1st (T)s	2nd (f)Hz	2nd (T)s
Ambient	Nov. 11, 2013	CH12	2.3439	0.4266	8.484	0.1179
		CH11	2.112	0.4735	8.484	0.1179
		CH10	2.3439	0.4266	7.4098	0.1349
		CH9	2.112	0.4735	8.484	0.1179
		CH8	2.3439	0.4277	7.422	0.1347
		CH7	2.3439	0.4266	7.361	0.1359
		CH6	2.3439	0.4266	7.422	0.1347
		CH5	2.112	0.4735	8.484	0.1179
		CH4	2.3439	0.4266	7.4098	0.1349

Table 3.2. Summarize the frequencies and periods obtained from all the 9-

channels in the building, from the ambient data recorded on Nov. 11, 2013

3.4.5. Analysis of an Earthquake Data Recorded on (Feb. 14, 2014)

In February 14, 2014 a moderate earthquake occurred in Antakya around 02:33am local time, (Figure 3.14 Koeri, 2014). The data recorded was processed and analyzed in MATLAB using Real-Time monitoring program. Figures 3.22-25 shows the plots of the Displacement of the building.

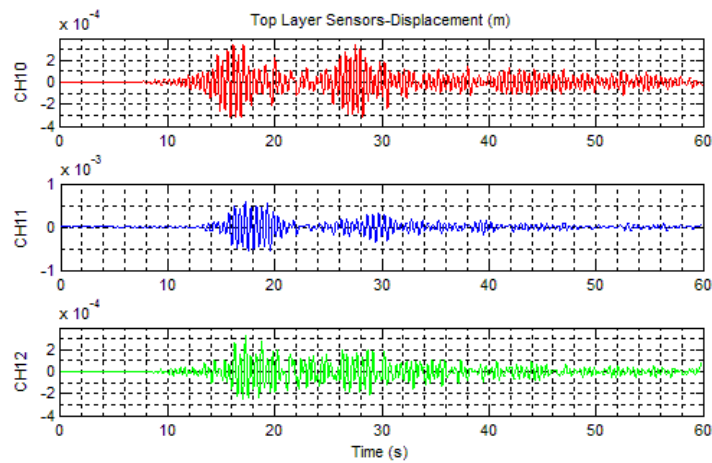


Figure 3.22. Displacement plot of the top three sensors (top layer) in meters

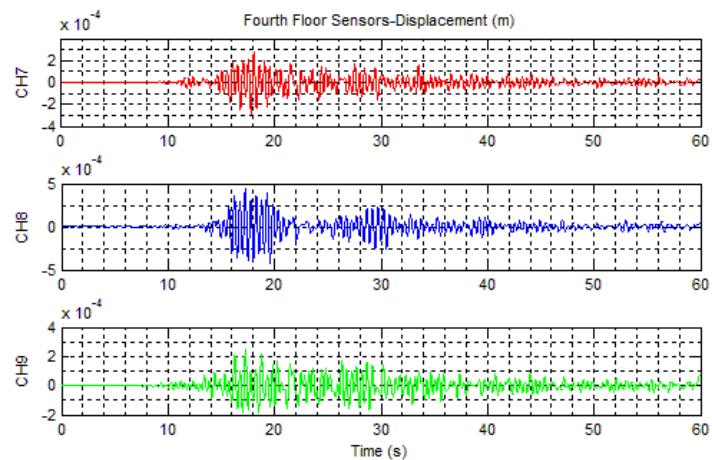


Figure 3.23. Displacement plot of the three sensors in the fourth floor, in meters

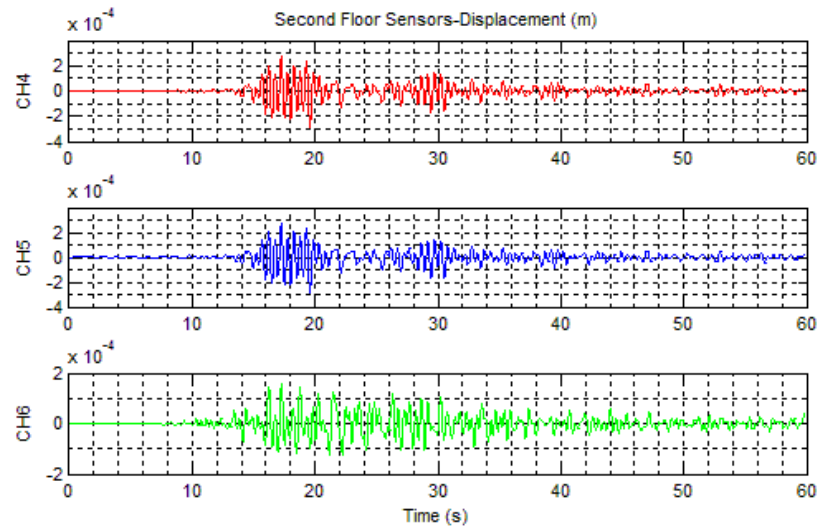


Figure 3.24. Displacement plot of the three sensors in the second floor, in meters

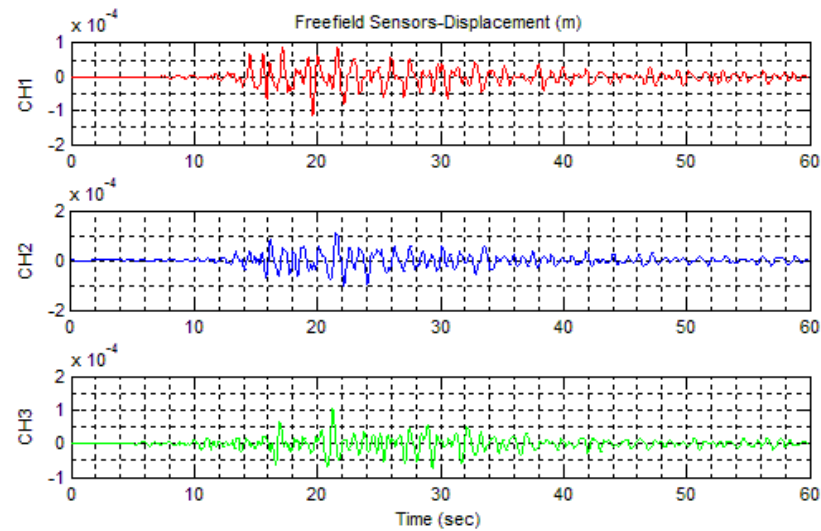


Figure 3.25. Displacement of the three sensors in the free-field station, in meters

Figures 3.26-28 shows the plots of the Fourier Amplitudes of the earthquake data, from all the 9-channels in the building.

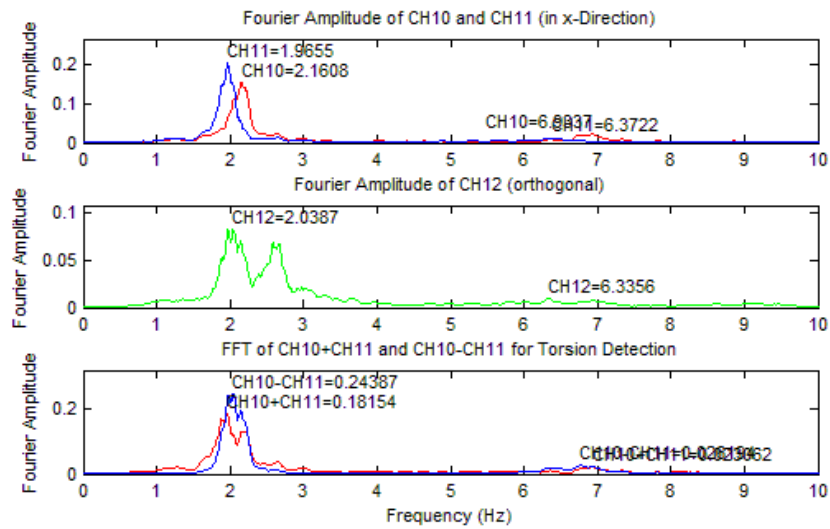


Figure 3.26. Fourier Amplitude plot of the top sensors, six floor (x-direction). The first plot is CH10 and CH11, the second plot is CH12. The third plot is (CH10+CH11) and (CH10-CH11) for torsion detection in the building

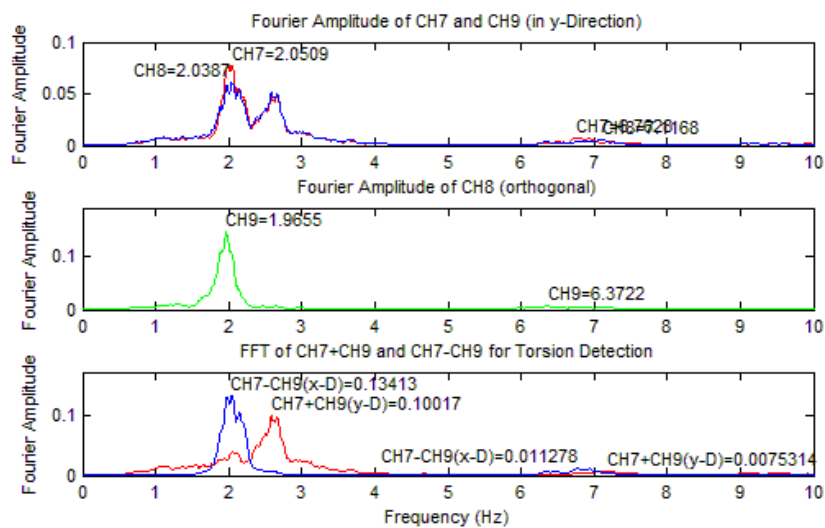


Figure 3.27. Fourier Amplitude plot of the sensors in fourth floor (y-direction). The first plot is CH7 and CH9, the second plot is CH8. The third plot is (CH7+CH9) and (CH7-CH9) for torsion detection in the building

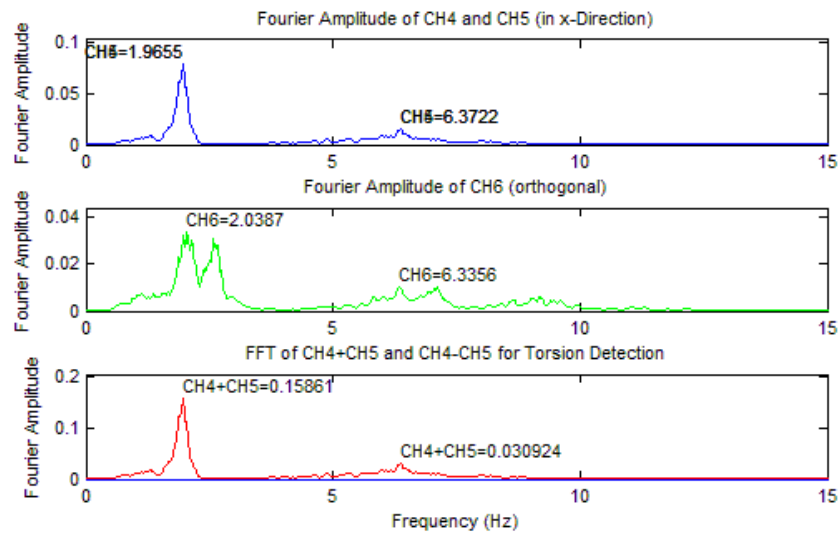


Figure 3.28. Fourier Amplitude plot of the sensors in second floor (x-direction). The first plot is CH4 and CH5, the second plot is CH6. The third plot is $(CH4+CH5)$ and $(CH4-CH5)$ for torsion detection in the building

Table 3.3. Summary of the experimental results obtained from the building, using earthquake data

Event type	Event date	Channel	1st (f) Hz	1st (T) s	2nd (f) Hz	2nd (T) s
Earthq.	Feb. 14, 2004	CH12	2.0387	0.4905	6.3356	0.1578
		CH11	1.9655	0.5088	6.3722	0.1567
		CH10	2.1608	0.4628	6.9337	0.1442
		CH9	1.9655	0.5088	6.3722	0.1567
		CH8	2.0387	0.4905	7.1168	0.1405
		CH7	2.0506	0.4877	6.7628	0.1479
		CH6	2.0387	0.4905	6.3358	0.1578
		CH5	1.9655	0.5088	6.3722	0.1567
		CH4	1.9655	0.5088	6.3722	0.1567

Table 3.3. Summarize the frequencies and periods obtained from all the 9-

channels in the building, from the moderate earthquake recorded on Feb. 14, 2014

3.4.6. Analysis of Ambient Data Recorded on (March 1, 2014)

In order to determine the effect of the earthquake in the building, an ambient data recorded on March 1, 2014 were processes and analyzed again, in MATLAB by using Real-Time monitoring program. Figures 3.29-35 shows the plots of the displacement of the building as well as Fourier Amplitudes plots.

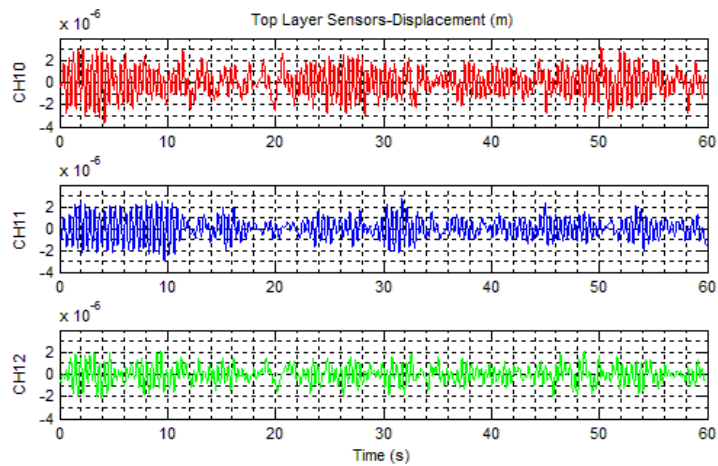


Figure 3.29. Displacement plot of the top three sensors (top layer) in meters

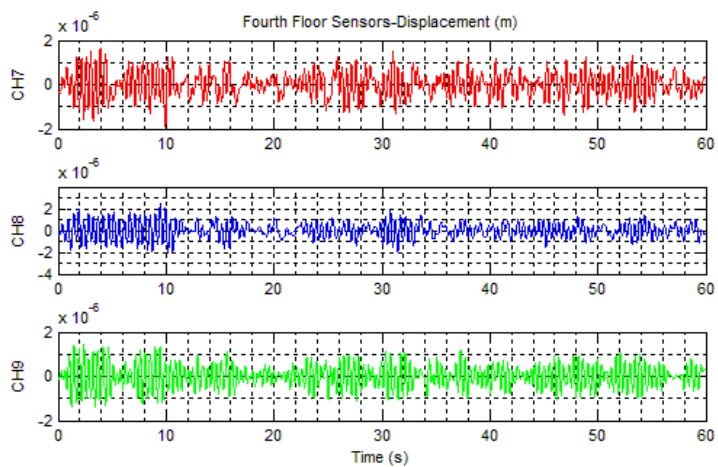


Figure 3.30. Displacement plot of the three sensors in fourth floor, in meters

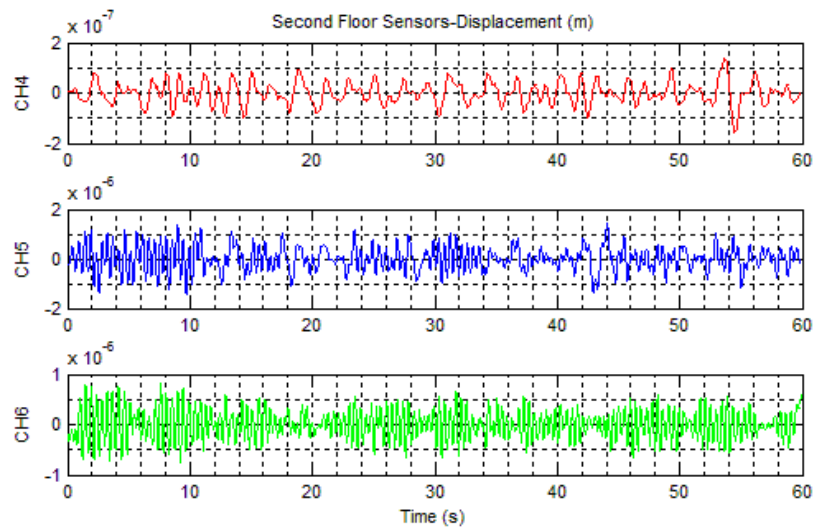


Figure 3.31. Displacement plot of the three sensors in second floor, in meters

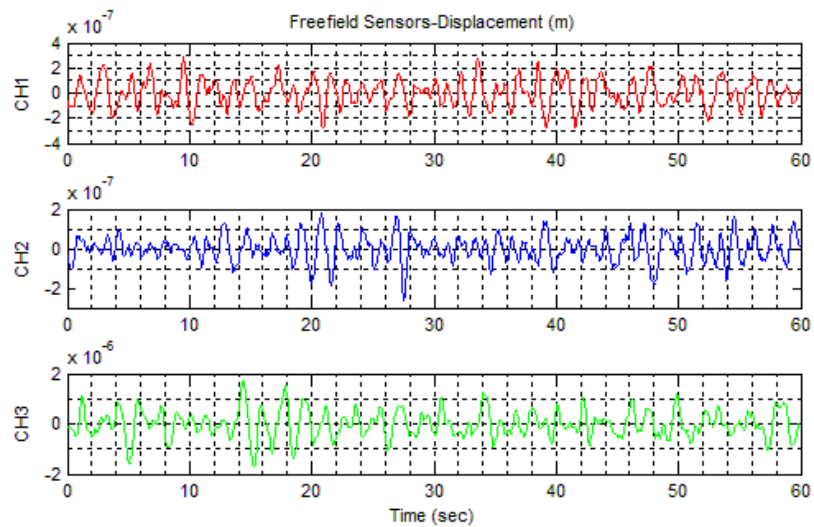


Figure 3.32. Displacement plot of the three sensors in free-field station, in meters

Figures 3.33-35 shows the plots of the Fourier Amplitudes of the ambient record, from all the 9-channels in the building.

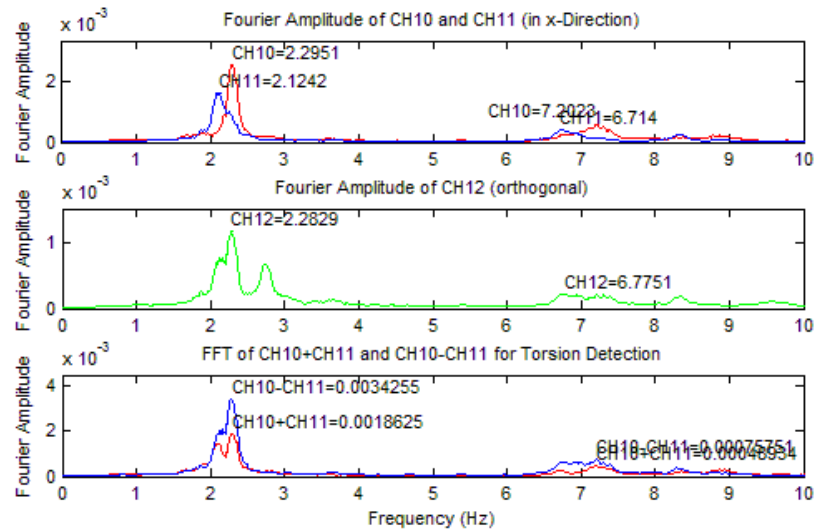


Figure 3.33. Fourier Amplitude plot of the top three sensors, sixth floor (x-direction).

The first plot is CH10 and CH11, the second plot is CH12. The third plot is (CH10+CH11) and (CH10-CH11) for torsion detection in the building

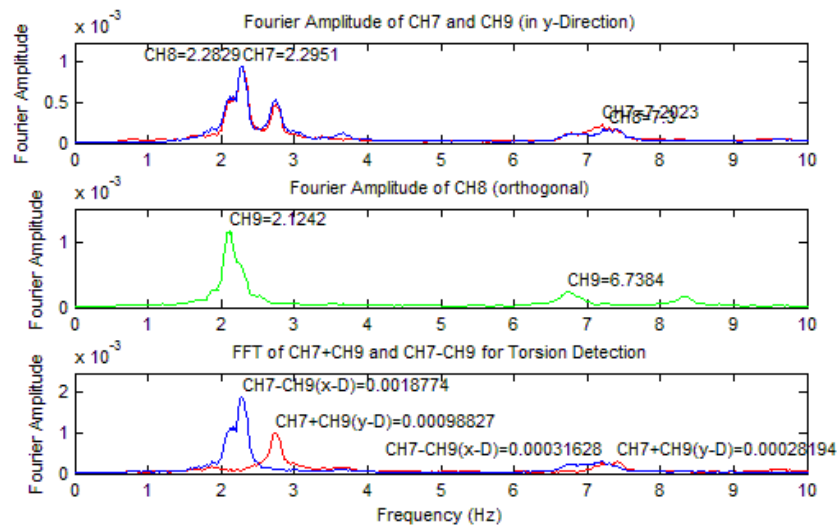


Figure 3.34. Fourier Amplitude plot of the sensors in fourth floor (y-direction). The first plot is CH7 and CH9, the second plot is CH8. The third plot is (CH7+CH9) and (CH7-CH9) for torsion detection in the building

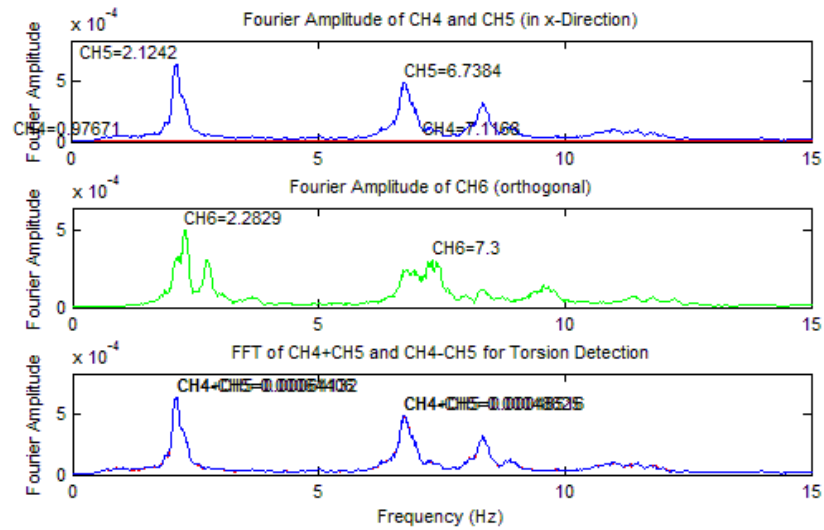


Figure 3.35. Fourier Amplitude plot of the sensors in second floor (x-direction). The first plot is CH4 and CH5, the second plot is CH6. The third plot is (CH4+CH5) and (CH4–CH5) for torsion detection in the building

Table 3.4. Summary of the experimental results obtained from the building, using ambient data

Event type	Event date	Channel	1st (f) Hz	1st (T) s	2nd (f) Hz	2nd (T) s
Ambient	March. 1, 2004	CH12	2.2829	0.438	6.7751	0.1476
		CH11	2.1242	0.4707	6.714	0.1489
		CH10	2.2951	0.4357	7.2023	0.1388
		CH9	2.1242	0.4708	6.7384	0.1484
		CH8	2.2829	0.438	7.4342	0.1345
		CH7	2.7467	0.3641	7.2145	0.1386
		CH6	2.7467	0.3641	6.8727	0.1455
		CH5	2.1242	0.4777	6.8727	0.1455
		CH4	1.111	0.9001	6.5553	0.1525

Table 3.4. Summarizes the frequencies and periods obtained from all the 9-

channels in the building from the ambient vibration reading, recorded on Feb. 14, 2014

3.5. Discussion of Experimental Results

Three different sets of data, were analyzed to better capture the vibration periods of the building. Two of the data were ambient records, and the third one is a medium earthquake record. The first ambient data is before the earthquake while the second one is after the earthquake in order to capture the differences in the vibration periods of the building before and after the earthquake. Table 3.5 summarizes the vibration periods of the building obtained from the three sets of data used in this project, from the top three sensors namely (CH10, CH11 and CH12) as well as the percentage differences between the recorded data.

Table 3.5. Summary of the experimental results obtained from the three sets of data

Channel	Amb. Data A		Earthq. Data B		Amb. Data C		(B-A)/A)	(B-C)/C)
	f(Hz)	T(s)	f(Hz)	T(s)	f(Hz)	T(s)		
CH12	2.3439	0.4266	2.0387	0.4905	2.2829	0.438	14.98%	11.99%
CH11	2.112	0.4735	1.9655	0.5088	2.1242	0.4707	7.46%	8.09%
CH10	2.3439	0.4266	2.1608	0.4628	2.2951	0.4357	8.49%	6.22%

From the table above the frequencies obtained from the building varies, from the ambient to earthquake readings, with little increase in period due to the following reasons.

- The flexibility nature of the steel building under earthquake lateral forces.
- Increase in the ground acceleration.
- The nature of the hinge connections between the steel members in the building (Stiffness Effect).

The percentage difference between the periods of the building Table 3.5 obtained

from the top three sensors in the building, is use to indicate the changes in the behavior of the building before and after the earthquake. By observing the differences in the periods obtained from the two ambient readings it is clearly indicating that there is no permanent damage in the building induced by the earthquake forces.

4. ANALYTICAL STUDY

4.1. Introduction

In this chapter an analytical model is used to simulate the measured dynamic properties namely (Frequency and Period) of the instrumented building in Antakya, Hatay. The model is carried out by using Sap2000 v16 version, one of the commonly used structural analysis (Finite Element) Program. The major calibrated parameters were selected to be floors mass, elastic modulus of both steel and concrete, infill walls, member locations as well as the strength of the concrete etc.

4.2. Finite Element Model (FEM)

The Finite Element Model of the building was constructed by using Sap2000 v16. The assumptions made in constructing the model are listed below:

- The structure is fixed at the basement
- All floors are rigid in their own plane (Rigid diaphragm assumption)
- Calculated story masses are lumped to the nodes defined at the geometric center of each story
- The steel members in the building was selected according to the Euro code, which are specified in the building details as (HE300A, HE240A) for Structural columns and (IPE200, IPE240, IPE300, IPE400, IPE450) for structural beams
- Shear walls were modeled by Mid-Pier Frame, and plastic hinges defined for nonlinear analysis, according to FEMA 356.
- Mid-Pier is modeled as a frame element with the shear wall cross sectional parameters.
- Brick walls were defined as an infill element, inform of strut model as a compression members (for walls without openings).
- For walls with opening, the brick walls were modeled as a refined continuum elements

The model is shown in the Figure 4.1

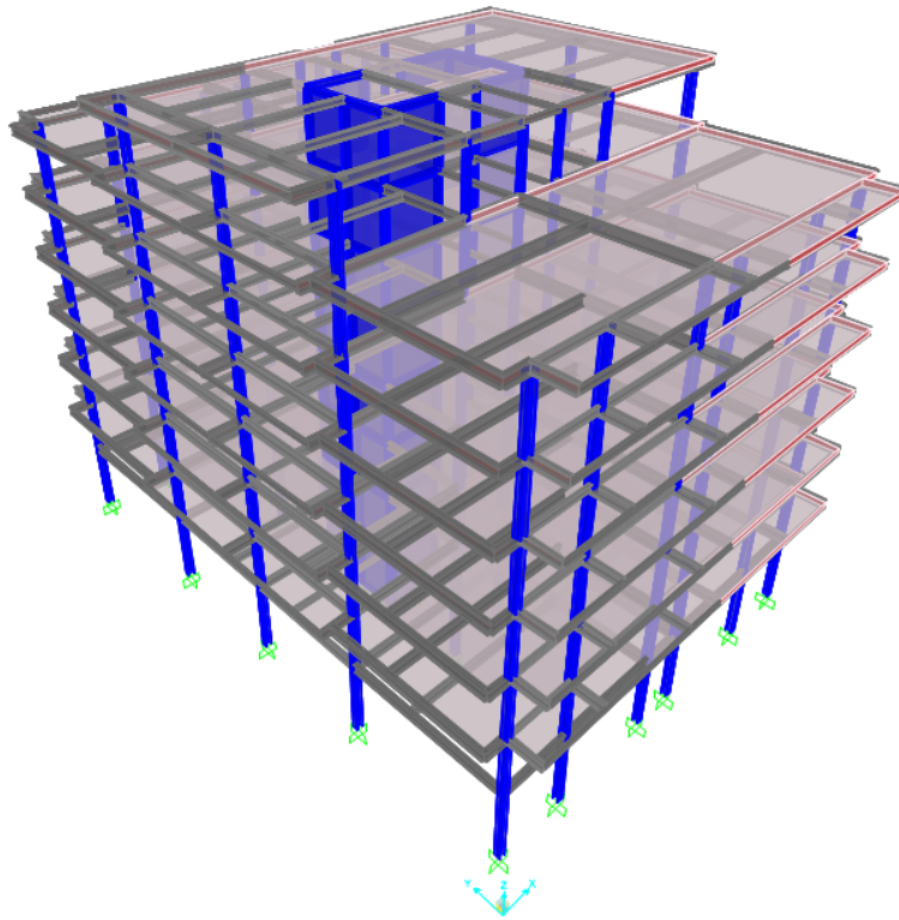


Figure 4.1. Three dimensional physical model of the instrumented building

Modal analysis was performed on the model and yielded the first three modal frequencies (periods) of the building in Table 4.1. The first mode is translation in x-direction, the second mode is translation in y-direction, and the third mode is torsional. The mode shapes are shown in the Figures 4.2. and 4.3.

Table 4.1. Summary of the modal analysis result obtained from the analysis model

Mode	Frequency (Hz)	Period (Sec)	Description
1	2.1234	0.471	x-Translation
2	2.4182	0.4135	y-Translation
3	7.6659	0.1305	Torsional

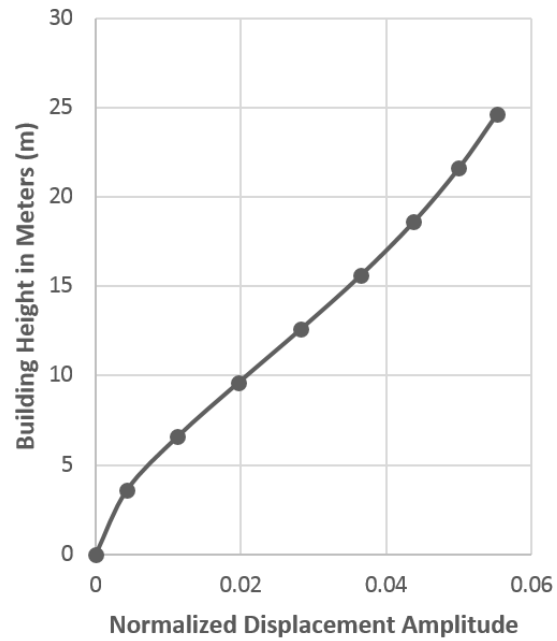


Figure 4.2. Fundamental mode shape of the instrumented building in y-direction

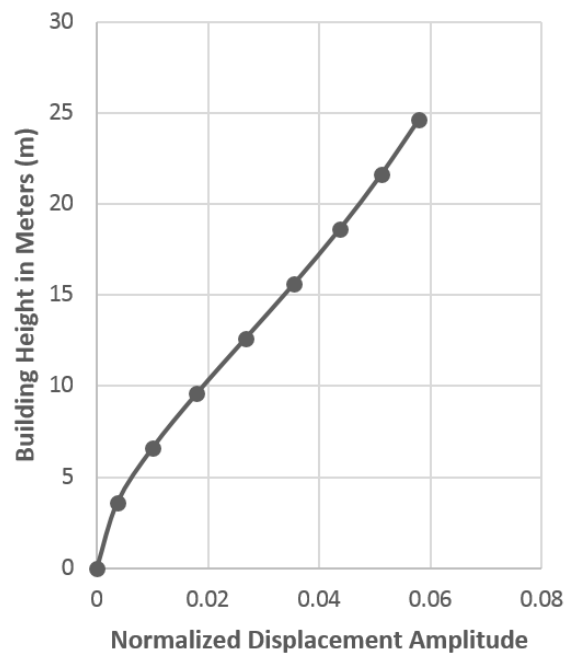


Figure 4.3. Fundamental mode shape of the instrumented building in x-direction

4.3. Comparison Between Experimental Results, Analytical Finite Element Model (FEM) and Code Formula

In Table 4.2. The fundamental periods and frequencies determined by Fourier analysis, FEM and Code formula are summarized. The fundamental period identified from the analyses of recorded data will provide an opportunity to compare it with the one obtained by the available empirical code formula. The comparisons will help in accessing the applicability of available empirical code formulas to estimate fundamental periods of structures.

In all buildings to which Equivalent Seismic Load Method is applied, the first natural vibration period may be calculated in accordance with section 6.7.4.3 of Turkish Earthquake Code as given in Equation 4.1.

$$T = 2\pi \left[\frac{\sum_{i=1}^N (m_i d_{fi}^2)}{\sum_{i=1}^N (F_{fi} d_{fi})} \right]^{1/2} \quad (4.1)$$

However, the first natural vibration period is permitted to be calculated by the approximate method given in section 6.7.4.2 of Turkish Earthquake Code as given in Equation 4.2.

$$T_1 \cong T_{1A} = C_t H_N^{3/4} \quad (4.2)$$

This empirical formula can be used for buildings with $H \leq 25\text{m}$ and located in the first and second seismic zones and also for all buildings to which Equivalent Seismic Load Method (ESLM) is applied in the third and fourth seismic zones. But in the case where $H > 25\text{m}$ and located in the first and second seismic zones, the application of

Equation 4.1 is mandatory.

For the case of this project the total height of the building is less than 25m i.e. $H < 25\text{m}$ and also it is located in first seismic zone. The application of approximate method is allow, the values of C_t in Equation 4.2 are defined as stated below and also depend on the structural system of the building.

- For buildings where seismic loads are fully resisted by reinforced concrete (R/C) structural walls, the value of C_t shall be calculated by the expression giving in Equation 4.3

$$C_t = \frac{0.075}{A_t^{0.05}} \leq 0.05 \quad (4.3)$$

Where A_t (Equivalent Area) is given by the expression in Equation 4.4. The maximum value of (L_{wj}/H_N) in Equation 4.4 shall be taken as equal to 0.9

$$A_t = \sum_j A_{wj} \left[0.2 + \left(\frac{L_{wj}}{H_N} \right)^2 \right] \quad (4.4)$$

- $C_t = 0.07$ for buildings whose structural system are composed only of reinforced concrete frames or structural steel eccentric braced frames
- $C_t = 0.08$ for buildings made of only structural steel frames
- And for the case (all buildings) the value of $C_t = 0.05$

For the case of the experimented steel building, the seismic resisting element comprises of two systems, the first one is the two central reinforced concrete (R/C) C-section walls facing each other at the center of the building, where one serve as the

elevator core and the other serve as the stair hall. The second one is the structural steel frames. Therefore, the value of C_t is considered as the general case or for all buildings i.e. $C_t = 0.05$. Table 4.2 summarizes the results obtained from the three different methods.

Table 4.2. Comparison of frequencies (Periods) from Fourier analyses, Finite Element Model and Code Formula

Methods	Frequency (Hz)	Period (s)
Fourier Analysis	2.1242	0.4707
Finite Element Model	2.123	0.471
Code Formula	1.8106	0.5523

From Table 4.2. The fundamental periods obtained from Fourier analysis and Finite Element Model (FEM) match well. But the obtained period from code formula differ with an increase in frequency. This is because of the code formula is a function of only the height of building and it is more conservative. Therefore, it is not taking into account the stiffness of the building.

4.4. Pushover Analysis

The pushover analysis can be used to evaluate the expected performance of a structural system by estimating its strength and deformation demands for design earthquakes by means of static inelastic analysis, and comparing these demands with available capacities at the performance levels of interest. In pushover analysis, the demands are estimated by the nonlinear static analysis of structure subjected to monotonically increasing lateral loading along a direction starting at the end of the gravity push [19]. The structure is pushed until either a predetermined target displacement [20] is reached or it collapse. The reliable post-yield material model and inelastic member deformations are extremely important in the nonlinear analysis. The evaluation is based on an assessment of important parameters, including global drift, inter-story drift, inelastic element deformations (either absolute or normalized with respect to a yield value),

deformation between elements, and element and connection forces (for elements and connections that cannot sustain inelastic deformations).

The nonlinear static pushover analysis can be viewed as a method for predicting seismic force and deformation demands, which accounts in an approximate manner for the redistribution of internal forces occurring when the structure is subjected to inertia forces that no longer resisted within the elastic range of structural behavior. The two key steps in applying this method, i.e. Lateral force distribution and target displacement are based on the assumption that the structure's response is mainly from the fundamental mode, and that the mode shapes remain unchanged after structure gets into the inelastic region.

The seismic performance of a building is measured by the state of damage under a certain level of seismic hazard. The state of damage is quantified by the drift of the roof and the displacement of the structural elements. There are two important features in performance evaluation of a buildings, i.e. demand and capacity. Demand is the representation of earthquake ground motion and the capacity is a representation of the structure's ability to resist the seismic demand. Performance is dependent on the manner that the building is able to handle the demand. The performance point of a structure, refers to the point where the demand curve intersect the capacity curve, it is the point that represent the global behavior of the structure Figure 4.4.

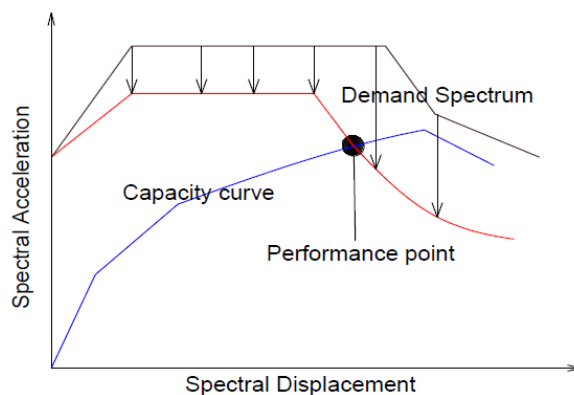


Figure 4.4. Performance point of a structure

4.5. Performance Levels of Structures and Elements

Building performance level is a combination of the performance levels of the structural and non-structural components. A performance level described a limiting damage condition which may be considered satisfactory for a given building and a given ground motion. The structural performance levels are designed using names and letters. The performance levels are discrete damage states, and identified from a continuous spectrum of possible damage states as given in Figure 4.5

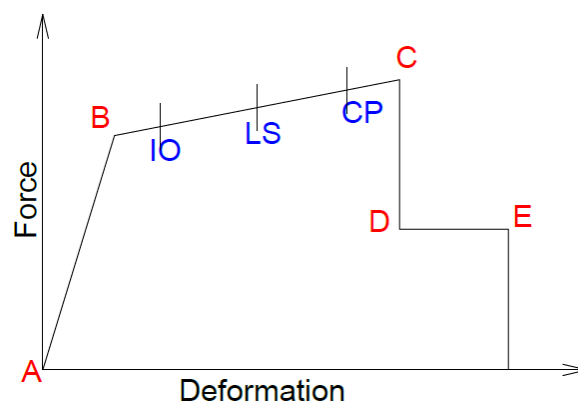


Figure 4.5. Performance levels as per FEMA 356

Figure 4.5. Represents the damage states as IO (Immediate Occupancy), LS (Life Safety) and CP (Collapse Prevention), respectively.

4.5.1. Immediate Occupancy (IO)

The structural performance level, which means that the post earthquake damage state in which only very limited structural damage has occurred. The basic vertical and lateral forces resisting elements of the building retain nearly all of their pre-earthquake strength and stiffness. Here, the risk of life threatening injury as a result of structural damage is very low. Although some minor structural repairs may be appropriate.

4.5.2. Life Safety (LS)

The structural performance level, life safety, means the post earthquake damage state in which significant damage to the structure has occurred, but some margin against either partial or total structural collapse remains. Some structural elements and components are severely damaged, but this has not resulted in large falling debris hazards, either within or outside the building. Injuries may occur during the earthquake, but the overall risk of life-threatening injury as a result of structural damage is expected to be low.

4.5.3. Collapse Prevention (CP)

The structural performance level, collapse prevention, means the post earthquake damage state in which the building is on the verge of partial or total collapse. Substantial damage to the structure has occurred, potentially including significant degradation in the stiffness and strength of the lateral force resisting system, large permanent lateral deformation of the structure, and to a limited extent of degradation in vertical load carrying capacity. However, all significant components of the gravity-load resisting system must continue to carry their gravity load demands. Significant risk of injury due to falling hazards from structural debris may exist. It may not be technically practical to repair the structural components and is not for re-occupancy, as aftershock activity could induce collapse.

4.6. Pushover Analysis of the Instrumented Building

The nonlinear static pushover analysis of the building was performed using Sap2000 (Version 16). The analytical model is shown in Figure 4.6. As mentioned earlier that the lateral resisting system of the building comprises of two system R/C walls and perimeter frames. Therefore for this case, the concrete shear walls was modeled by using Mid-Pier frame with plastic hinges defined according to FEMA 356. The Mid-Pier is modeled as a frame element with the shear wall cross sectional parameters. The thickness of the rectangular rigid beam section is considered as the same as the wall

itself (Figure 4.7). The axial force level is considered from the combination of the dead and live loads ($D + 0.3L$) and the transverse reinforcement is assumed not to provide confinement.

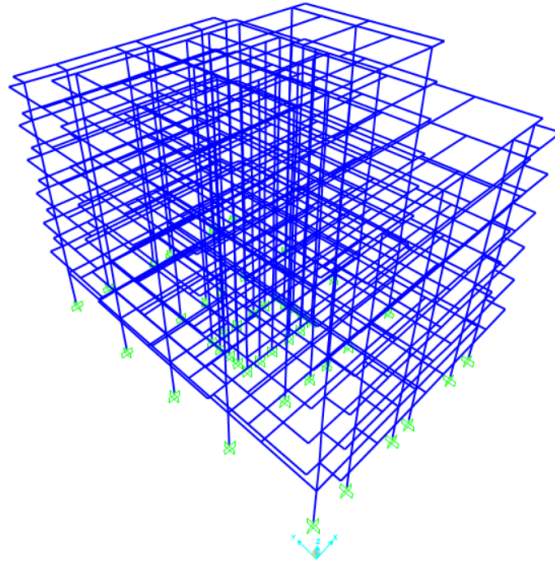


Figure 4.6. Three dimensional analytical model of the instrumented building

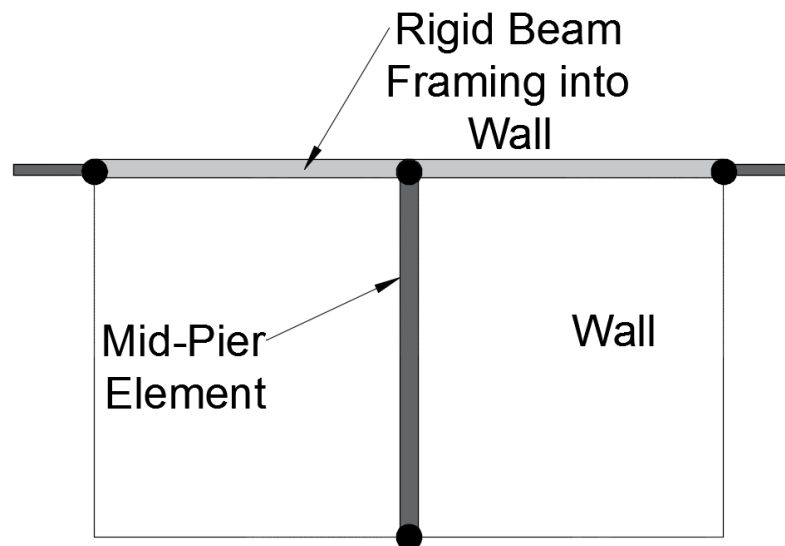


Figure 4.7. Mid-Pier model for shear wall

Since from the modal analysis, the first dominant mode of the structural model

were in x-direction, the analytical model was pushed 20cm at joint 730 in positive and negative x-directions. The period of vibration is larger in x-direction than in y-direction, hence the stiffness in the x-direction is lower than the y-direction.

During these analyses the mass center of the roof story was chosen as the control node for each story. Lateral loads were applied to the model with an increasing uniform distribution from roof story to the ground story. During the pushover analysis, the magnitude of the control node's displacement was increased and the sequence of cracks, yielding, plastic hinges formations and failure of various structural components were calculated by the analysis software.

During the analysis, the structure will reach a limit state or collapse condition. This will allow the software to stop pushing the analytical model of the structure and the total applied shear force and associated lateral displacement at each increment was plotted automatically and it is called pushover curve (Capacity Curve). The pushover curves for the building in x-directions, story drift, performance point and plastic hinges formations are shown in Figures 4.8-11. Respectively.

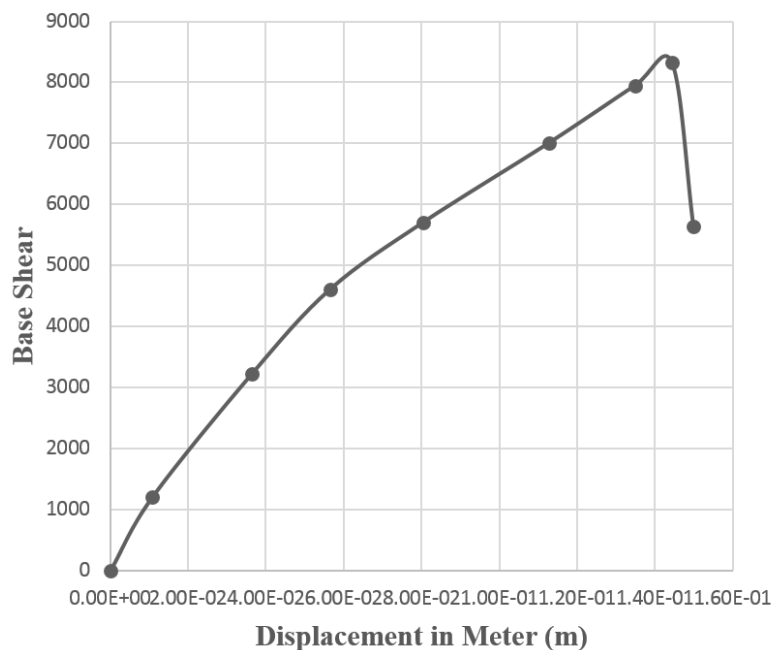


Figure 4.8. Pushover curve of the instrumented building

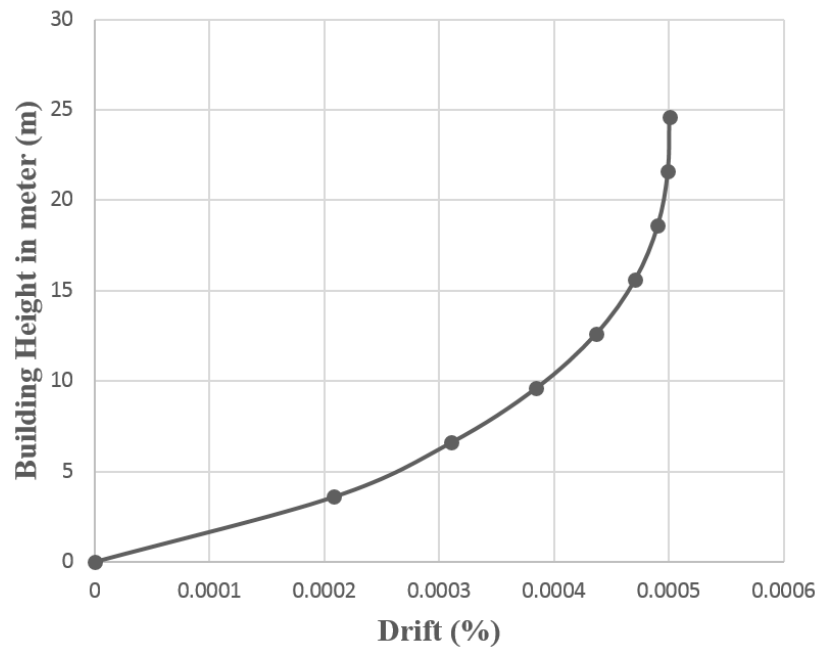


Figure 4.9. Story drift ratio of the instrumented building

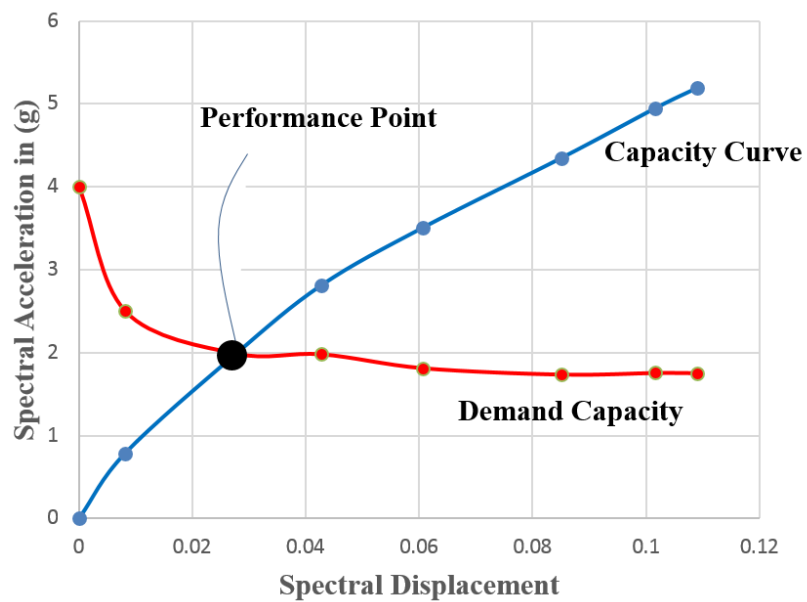


Figure 4.10. Performance point of the instrumented steel building

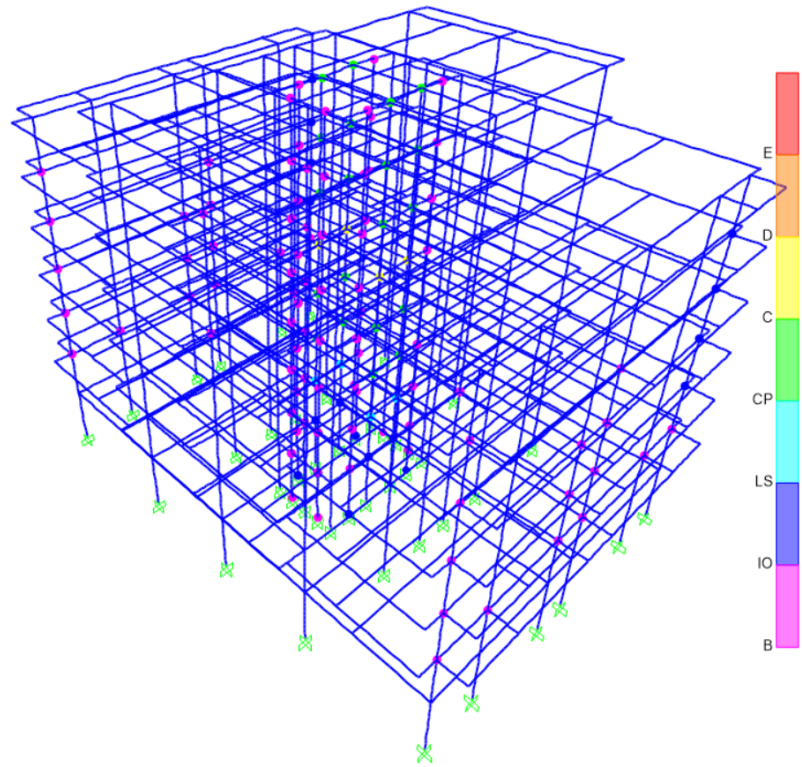


Figure 4.11. Plastic hinges of the instrumented building in x-direction

From the intersection of demand curve and capacity curve (performance point) in Figure 4.10. It is the point that represent the global behavior of the building, the building period is found to be (0.2356s) which correspond to the step 3 and 4 of the pushover analysis. The hinges formations were checked in step 3 and 4 (Figure 4.11). The largest formed hinges are at the immediate occupancy level. Since the performance point of the building stayed in the linear range of the capacity curve, this is indicating none of the elements on the model reached yield point. Therefore, according to the analysis results, the instrumented steel building is expected to show a good performance under earthquake conditions.

5. CONCLUSIONS AND RECOMMENDATIONS

5.1. Summary

A 6-story, steel building with reinforced concrete (R/C) core shear walls, were instrumented with 12 uni-axial accelerometers, which is intended for Structural Health Monitoring (SHM) system with aims of providing in real-time informations regarding the health of the building. The transducers were used to continuously take readings at 100Hz and triggered readings at 200Hz. All the setups, outputs and configurations of the monitoring system were controlled by Scream Software. Remote connection was established using internet connection between our local computer at Zirve University and the data logger's computer in the instrumented building. The response of the building to ambient vibrations from ground and wind were recorded by the sensitive accelerometers continuously.

From the continuous readings recorded, three different readings was selected and analyzed by using Fast Fourier Transform in Matlab, two of them are ambient readings and the third one is earthquake reading with moderate magnitude. The natural frequencies and periods obtained from the instrumented building were compared with each other in order to investigate the effect of earthquake in the building.

A 3D-Finite Element Model (FEM) of the instrumented building was prepared and analytical results obtained from modal analysis were compared with the experimental results and the code formula. Nonlinear pushover analysis was performed on the analytical model and the pushover curves and the performance point were obtained. The performance point showed that the structure will perform well under earthquakes shaking.

The results obtained from the study can be used to improve the design and construction technology of steel buildings, and contribution to the ongoing researches, as well as reducing the loss of lives and properties during an earthquakes.

5.2. Conclusions

In this study majority of the previously defined objectives were achieved, including an ability to instrument the steel building and monitoring the building in real-time, and storing the recorded data. Post processing of ambient and moderate earthquake dynamic readings was successfully obtained and frequencies and periods of the instrumented building were obtained under different readings. The comparison between the obtained results from the recorded data showed that there is no damages resulting from the recent earthquake on the monitored building. Finite Element Model (FEM) of the instrumented building were performed by using SAP2000 software, the natural frequency and period were obtained from the analytical model were compared with the experimented results as well as the code formula for finding the first vibration period of the building located in earthquake regions. Also the performance point obtained from the instrumented building by using pushover analysis, it is indicating that the building will show a good performance under earthquake shakings.

5.3. Recommendations

- Result obtained from this study indicate the importance of Structural Health Monitoring (SHM) system or Seismic instrumentations of building in determining the dynamic properties of a building
- The results obtained from the two ambient readings and the moderate earthquake reading, such monitoring system may be required in monitoring the health of the building structures
- Structural Health Monitoring (SHM) may be used to capture structural conditions and performance levels of a building, before, after and during the earthquake. Hence comparing the dynamic properties may indicate if there are any permanent structural damage in the building
- A Structural Health Monitoring (SHM) systems would be recommended for important structures, thereby reducing the loss of lives and properties

REFERENCES

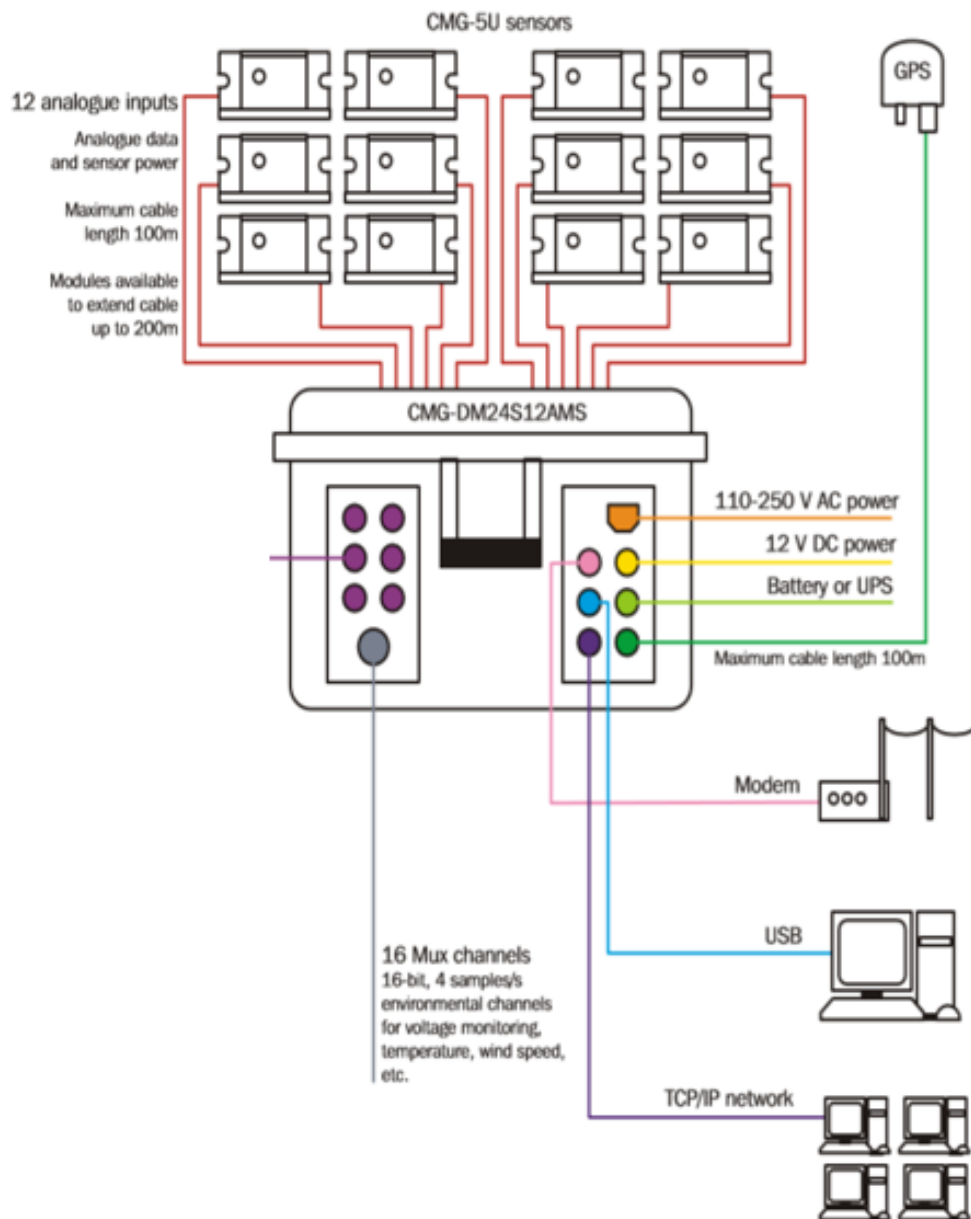
1. Lynch, J. P. and K. Loh J. “A Summary Review of Wireless Sensors and Sensor Networks for Structural Health Monitoring”, *Shock and Vibration Digest*, vol. 38, no. 2, pp. 91–130, 2006.
2. Ellsworth, W., C. Mehmet, J. Evans, E. Jensen, R. Kayen, M. Metz, D. Nyman, J. Roddick, P. Spudich, and C. Stephens, “Near-Field Ground Motion of the 2002 Denali Fault, Alaska, Earthquake Recorded at Pump Station 10”, *Earthquake Spectra*, vol. 20, no. 3, pp. 597–615, 2004.
3. Celebi, M. “Seismic Instrumentation of Buildings (with Emphasis on Federal Buildings)”, *Special GSA/USGS Project, an Administrative Report*, 2004.
4. kinometrics, “<http://www.kmi.com/p-87-EpiSensor-ES-T.aspx>”, *Innovative World Leader in Earthquake Monitoring*, February, 2014.
5. REFTEK, “www.reftek.com/products/motion-recorders-130-SMA.htm”, *Manufactures Seismometers, Seismic Recorders, Motion Recorders and Accelerometers for Seismic and Earthquake Engineering Systems*, February, 2014.
6. Seismograph, “www.expins.com/item/geode-seismograph”, *Exploration Instruments LLC*, February, 2014.
7. Lynch, J. P. “An Overview of Wireless Structural Health Monitoring for Civil Structures”, *Philosophical Transactions of the Royal Society A: Mathematical, Physical and Engineering Sciences, The Royal Society*, vol. 365, no. 1851, pp. 345–372, 2007.
8. Celebi, M., M. Sereci, R. Boroschek, R. Carreño, and P. Bonelli, “Identifying the Dynamic Characteristics of a Dual Core-Wall and Frame Building in Chile Using Aftershocks of the 27 February 2010 (Mw= 8.8) Maule, Chile, Earthquake”,

- Earthquake Spectra, Earthquake Engineering Research Institute*, vol. 29, no. 4, pp. 1233–1254, 2013.
9. Celebi, M., N. Toksöz, and O. Büyüköztürk, “Rocking Behavior of an Instrumented Unique Building on the MIT Campus Identified from Ambient Shaking Data”, *Earthquake Spectra, Earthquake Engineering Research Institute*, 2013.
 10. Celebi, M., M. Huang, A. Shakal, J. Hooper, and R. Klemencic, “Ambient Response of a Unique Performance-Based Design Tall Building with Dynamic Response Modification Features”, *The Structural Design of Tall and Special Buildings, Wiley Online Library*, vol. 22, no. 10, pp. 816–829, 2013.
 11. Naeim, F., “Performance Analysis of a Damaged 11 Story Steel Moment Frame Building During the 1994 Northridge Earthquake”, *Proc. of the 11th World Conference on Earthquake Engineering, Paper*, vol. 1428, 1996.
 12. dlubal, “<http://www.dlubal.com/>”, *Finite Element Analysis Software*, March, 2014.
 13. Over, S., A. Buyuksarac, O. Bekta, Ozcan and A. Filazi, “Assessment of Potential Seismic Hazard and Site Effect in Antakya (Hatay Province), SE Turkey”, *J. Environ. Earth Sci., Springer*, vol. 62, no. 2, 2011.
 14. De Silva, C. W., *Vibration: Fundamentals and Practice*, CRC Press, 2006.
 15. KOERI, “<http://www.koeri.boun.edu.tr/scripts/lasteq.asp>”, *Kandilli Observatory and Earthquake Research Institute, National Earthquake Monitoring Center (NEMC) Turkey*, February, 2014.
 16. Brigham, E and R. Morrow, “The Fast Fourier Transform”, *Spectrum, IEEE*, vol. 4, no. 12, pp. 63–70, 1967.
 17. Cooley, J. W. and J. W. Tukey, “An Algorithm for the Machine Calculation of Complex Fourier Series”, *Math. Comput.*, vol. 19, no. 90, pp. 297–301, 1965.

18. Steven, C. C. and P. Raymond, “Numerical Methods for Engineers with Programming and Software Applications”, *WCB/McGraw-Hill*, pp. 719–744, 1998.
19. Shuraim, A and A. Charif, “Performance of Pushover Procedure in Evaluating the Seismic Adequacy of Reinforced Concrete Frames”, 2007.
20. Council, Building Seismic Safety, “Prestandard and Commentary for the Seismic Rehabilitation of Buildings”, *Report FEMA-356, Washington, DC*, 2000.
21. Cinitha, A., P. Umesha and I. Nagesh, R., “Evaluation of Seismic Performance of an Existing Steel Building-Pushover Analysis Approach”, 2010.
22. Chopra, A. K. and R. K. Goel, “A modal Pushover Analysis Procedure for Estimating Seismic Demands for Buildings”, *Earthquake Engineering and Structural Dynamics*, vol. 31, no. 3, pp. 561–582, 2002.
23. Sohn, H., C. Farrar, R., F. Hemez M., D. Shunk, D. W. Stinemates, R. Brett, and J. J. Czarnecki, “A Review of Structural Health Monitoring Literature: 1996-2001”, *os Alamos National Laboratory Los Alamos, NM*, 2004.
24. Emel, D., *3D-FE Model Field-Calibration and Rating Studies on Existing Reinforced Concrete Building*, M. Sc. Thesis, Middle East Technical University, 2006.
25. Ozan, C. C. *Forced Vibration Testing of Existing Reinforced Concrete Buildings*, M. Sc. Thesis, Middle East Technical University, 2006.

APPENDIX A:

Array layout for a typical CMG-DM24S12AMS



- Power Can be Supplied to the system using mains or batteries, which can be optionally recharged when mains power is available
- The built-in PC includes Ethernet, USB and internal modem connectivity options